# Computational analysis of fluid flow in an annulus for the drilling of oil and gas wells

**By**

**Shah Fahad**

**School of Chemical and Materials Engineering (SCME)**

**National University of Sciences and Technology (NUST)**

**2018**

# Computational analysis of fluid flow in an annulus for the drilling of oil and gas wells

Shah Fahad
NUST201463867MSCME67814F

**This work is submitted as a MS thesis in partial fulfillment of the requirement for the degree of**

**(M.S in Chemical Engineering)**

**Supervisor Name: Dr. Muhammad Ahsan**

**School of Chemical and Materials Engineering (SCME)**
**National University of Sciences and Technology (NUST),**
**H-12 Islamabad, Pakistan**

**July, 2018**

# DEDICATION

MY THESIS IS REAL SUCCESS OF MY PARENT'S PRAYERS, MY SUPERVISOR, BILAL HUSSAIN AND MY OTHER FRIENDS

# Acknowledgments

All the praises for Allah, which can't be described by us the speakers, HIS blessings aren't measured through computation, whom the altitude of logical nerve can't escalate, and the depths of understanding can't be achieved; HE has no limits to be described in any means, no eulogy occurs, no time is intended, and no extent is static. Countless salutation upon "HOLY PROPHET HAZRAT MUHAMMAD (S.A.W.W.)."

I hereby acknowledge and present my earnest appreciation to my research supervisor, Dr. Muhammad Ahsan to support me at every level, supervision & meaningful guidance to direct me in a very accurate way whenever I asked for. I wouldn't hesitate to pay my appreciation to the members of GEC, including Dr. Iftikhar Ahmad & Dr. Sarah Farrukh aimed at their valuable suggestions & guidance.

It is most important to also include the names of Dr. Arshad Hussain (Principal, School of Chemical and Materials Engineering) and Dr. Bilal Niazi (HOD, Department of Chemical Engineering) for providing a research-oriented platform to utilize my skills in accomplishing this research work effectively.

In the end, all my achievements & this work is dedicated to my parents, because without their endless support & countless prayers, I stand nowhere in my life. Where I am today wouldn't be possible deprived of my parents' existence.

*Shah Fahad*

# Abstract

An annulus having 0.5 eccentricity, with the diameters ratio of 0.5, measuring three velocity elements consisted of feebly fluid deprived of non-Newtonian shear thinning elasticity and rotational inner cylinder at 300rpm. At laminar region of flow, concerned by 0.2% solution of CMC (Sodium carbo methyl cellulose), based on polymer, it was observed that near the outer pipe wall, a counter rotating flow was observed which was not evidenced at 9200 Reynolds number. The Non-Newtonian fluid will depict the same effects of rotation having more even axial flow through the annulus alike with the simulated work. In all the cases the maximum tangential velocities will be found in the thinnest gap. With the extreme values of bulk velocities near the inner pipe, the secondary flow circulation with the Newtonian fluid at various Reynold's No. will be found in the direction of rotation. The rotation did not influence due to turbulence moderations & in the smallest gap region, Non-Newtonian fluid will decrease. At low Reynolds numbers, the flow resistance of both fluids will be raised with rotation & with the analogous of non-rotating flow resistances will also be reduced by increasing Reynolds no. For the same Rossby number, the tangential velocities will be found equal. Numerical simulation for the transportation of cuttings in drilling of oil wells, based on the sliding mesh for rotational pipe with the analogous of grainy flow on the kinetic theory basis. The comportment of the drilling fluid was relied on the power-law model. By comparing the outcomes with the literature experimental data, it has been evidenced that impact of rotated inner pipe follows the similar trend as originated in the experimental data.

**Keywords**: Rotational annular Drill-pipe; Non- Newtonian shear thinning fluid; Eccentrically configured annuli; Mathematical modelling

# Table of Contents

# Table of Figures

# List of Tables

# Abbreviations

$D_{in:}$ inner cylinder diameter (mm)

$D_{o:}$ outer pipe diameter (mm)

Rs: Rossby number

$d_{h:}$ hydraulic diameter (mm)

Re: bulk flow Reynolds number

S: inner and outer wall gap (mm)

e: eccentricity

uv: Reynolds shear stress ($m^2/sec^2$)

$R_{in:}$ Inner cylinder radius (mm)

$R_o$: Outer pipe radius (mm)

$\mu_{w:}$ Effective viscosity ($Kg.m^{-1}.sec^{-1}$)

ρ: Density of the drilling fluid ($Kg.m^{-3}$)

$\omega_d$: rotational speed of drill pipe (rpm)

V: Volumetric flowrate ($m^3.sec^{-1}$)

$G_m$: Mass flowrate ($Kg.sec^{-1}$)

$U_b$: bulk velocity ($m.sec^{-1}$)

$C_d$: coefficient of drag

g: acceleration due to gravity

k: kinetic energy for turbulence

K: factor of consistency ($Pa.s^n$)

ν: velocity vector

ε: volumetric concentration

β: drag coefficient

Ƭ: tensor of stress

n: power- law index

η: apparent viscosity

ϒ: shear rate

$\mu_s$: shear viscosity of solid

ω: Specific dissipation rate

ϕ= energy exchanged among the fluids

CMC: Sodium carbo methyl cellulose

Re: Reynolds number

Gi: gap between outer and inner wall in an eccentric anulus (mm)

Li: Radial length from inner to outer wall cylinder (mm)

L: inner and outer pipe center to center distance (mm)

# Chapter 1

# Introduction

## 1.1 Background

Energy stored as an underneath heat of solid surface of earth is known as the Geothermal energy. About 30% of outstanding heat of aforesaid energy is disbursed during the earth foundation and the kinetic energy related to agglomeration was the basis of such outstanding heat and concerned estimated time was around 5 milliards years ago for the earth formation. Rest of 70% energy is produced from the decay of radioactive isotopes of uranium 235, potassium 40, thorium 232 & uranium 238. Such materials generate the heat beneath the earth on unceasing basis [1]. Its harsh to say but geothermal is not the energy with renewable form. Nevertheless, it can fulfill the demand of the humans for thousands of years despite of the nuclear energy and the fossil fuels whose quantity is more prone to be finished in upcoming time. Since 2.6 million of years ago (Paleolithic era), geothermal energy has been allocated by the manhood, generally on such places where promising environments are occurred. Such of the places are classified through the shrill coated earth comprised of the permeable and warm formations of geology accompanied by the aquafers hence warm water obtainable at the surface in effortlessly. Usually these are originated in the regions of dynamic volcanic zones, such as USA, Iceland, Russia etc. Warm water springs are also obtainable on other sites and is utilized as the heating of houses or as the hot bath. By the deep well bores it is conceivable to grasp the aquafers, if not found near the surfaces. Such resources are odd to be found and are known as hydrothermal systems. Normally, geothermal energy is found I in less expediently sites in the spread of current technology of drilling wells. Principally through formations of low permeability, numerous ingenuities are emerging new technologies for the extraction of geothermal energy. These are termed as HDR or Hot Dry Rock, petrothermal, HWR or Hot Wet Rock, HFR or Hot Fractured Rock and EGS or Enhanced systems of geothermal. Entailment of deep well bores is needed, if any of volcanic regions are not near, such resources can be petrothermal or hydrothermal [2].

The creation of such well bore is planned to create formations with natural crack system for the assurance of the production to raise the underground heat transfer

surface. Also, non-natural cracking is also probable in the absence of such process. In the oil and gas industry, existing drilling technology is being conformed. The aim of the oil and gas well bores are to link the surface facilities with the natural mineral deposits after the phase of exploration.

## 1.2 Construction of Oil and gas wells

Cementing a series of steel casings in the development of the oil and gas wells is necessarily accompanied as the depth of the well is increased. It has objective to provide the isolation on zonal basis through the whole length of the well and for backing of the wellbore by the assurance of hydraulic seal on the outer side of the casing to prevent contamination [3].

In the primary cementing process, when the new section of well has been drilled, leaving the mud in the wellbore, the drilling pipe is withdrawn from the wellbore. Steel casing segment is then implanted into the bore, a gap of about 2cm is left in annulus (among the rock and the outside of the casing). To avoid tumbling of steel casing in the wellbore, centralizers are occasionally installed to the outside of the casing and in common practice, such gap of annuli becomes eccentric. Numerous fluids are pumped into the tubing when the casing has been placed, such fluids reach the bottom and return to the surface by the annular gap of casing and wellbore. Classically, for the displacement of resident mud cleaning, which has been left in between the annulus is accomplished by means of spacer fluid convoyed by one or more slurries of cement. Circulation is halted a few meters has been left in the casing at the bottom, drilling mud follows the slurry of cement pumping. Afterwards, cement is now allowed to set firmly. Furthermore, the drilling is continued by the residual cemented section inclusive of the casing and then in the prime rock formation [4].

By the elimination of spacer fluid and the mud through the annuli by the slurry of cement, a efficacious cementing job is occasioned. Inadvertently, migration of gases and liquids is possible in upward directions from the nearby formations of rock due to porous channeling, which are produced because occasionally mud is left behind in the annulus portions and after the setting of cement when water is detached, such problem arises. It may cause the loss of production due to spoliation of the environment and safety. Expensive jobs of squeeze cementing are then essential for the rectification of such trouble [5]

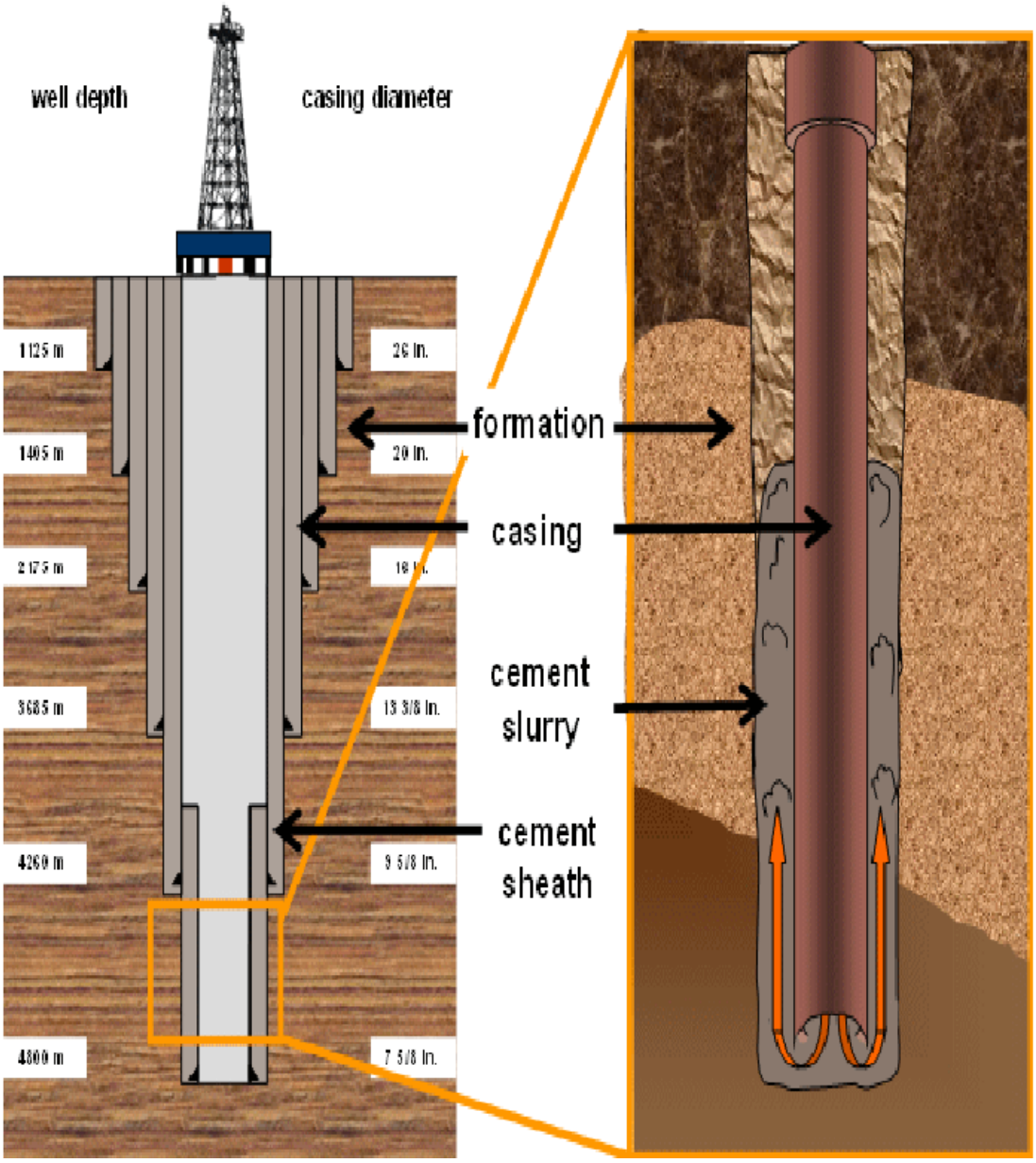


Figure 1 Drilling & cementing in Oil & Gas wells

## 1.3 Problems Encountered in Cuttings Transport

Cutting can be defined as the removal of drilled material while construction of a well. These cuttings usually create the hole and bottom of this hole can be in direct contact with the drilling bit. This very process takes place when drilling fluid can be pumped down via the drill pipe to drill bit and the same drilling fluid bears the responsibility to control the pressure inside the well and cooling of drill bit, while flowing upwards through the annulus space between the drill pipe and walls of the well.

It is difficult to monitor the drilling operation overall with the aid of measuring equipment due to severe conditions inside the well-bore. To overcome this difficulty, progress of a process is monitored by adapting the modelling approaches to characterize the process with the provision of necessary information.

Conventionally, to define operational parameters, steady-state models are considered which are purely based on empirical correlations[6]. The main purpose of these models is to determine a minimum transport velocity and the relevant friction losses. The suggested operating velocity is predicted to be within the range of 2 to 6 times the settling velocity of large particles [7].

Moreover, to represent the proper transport conditions, it is required to understand the phenomena which affects the transport conditions.

The efficiency of the drilling operations is based upon interaction processes where drilling fluid plays a major role. To meet the today's requirements, High Pressure-High Temperature conditions when drilling even below 6500 m, makes drilling more complex and challenging because at such conditions imparts the considerable change in properties of drilling fluid and therefore it is difficult to clean the hole.

In contrary, there is an absence of more suitable and accurate models in defining the transport characteristics of cuttings in directional drilling. Therefore, cutting beds may create more risk of potential clogging. Risk of clogging in larger time scales, is due to penetration at different rates and intermediate processes, whereas in small time scales, it is due to unsteady flow [8]

### 1.3.1 Accumulation Problem during drilling:

To undergo successfully the hole-cleaning process, it is necessary to increase the flow of drilling fluid, which will ultimately decrease the cuttings conc. in the annular region. It's also important to consider that high velocity is limited to surface equipment and down-hole drill string, as well as erosion to the hole and uncontrolled losses are also occur due to high velocities [9].

An inclination greater than 30degrees is prone to be created during the drilling of the well and a bed of cuttings starts forming. Pipe stuck problem arises when the weight on the drill bit is decreased which causes Rate of penetration in a decreasing trend, these problems are consequences of the scenario when the inclination of cutting bed is

likely to be deformed to slide among the inclinations of 30 to 60 degrees. Consequently, severe damage of drilling pipe is occurred, which may result in globular circumstances loss, additional price of mud additives and the loss of time and the production curtailment. It can be depicted in figure (2)

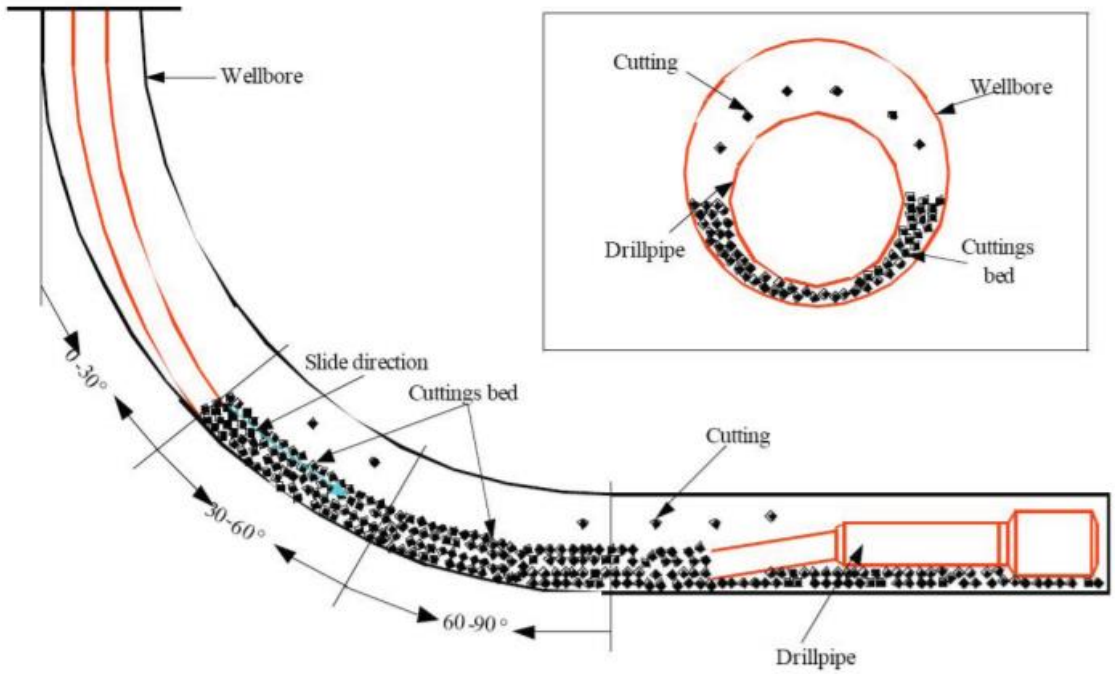


Figure 2 Accumulation problems during drilling

## 1.4 Route of the well: Large scale model

To represent the complete well-bore in large scale modelling, following objectives are considered;

a) To study different accident and broader vision of safety implications.

b) To develop & design the relevant devices.

c) To optimize the operational basis.

d) To control the process via simulation.

The input characteristics of industrial model are followed as;

1) flow rates. 2) Drilling fluid & its properties. 3) Consideration of the amount of carried solids. 4) Valid Temperature Profile. 5) Methods of hole cleaning.

The output characteristics of such model are; 1) Velocity of different phases. 2) Pressure distribution. 3) Temperature distribution of fluids. 4) Height of bed [10].

1-D transient transport models are coupled with thermal models are considered in the overall transport processes inside the well in large scale model. The temperature distribution profile of formation is also important. Both the diffusive and convective transport are considered through bi-directional coupling of transport and thermal model. DFM (Drift Flux Model) is utilized in determination of transport in dispersed phase. It is important to note that friction factor is also required to consider the viscous effects in well-bore [11].

## 1.5 Diameter of Particle: Small Scale

It is important to specify drag and lift coefficients at this small particle scales. In order to determine the settling velocities, it is necessary to specify drag of particles in large and small-scale models. Whereas to entrain the particles in deviated sections of the well-bore, lift forces are required to quantify the particles distribution.

The input characteristics to this model is as; 1) Non-Newtonian flow deformation 2) Distribution of particles of different sizes. 3) Shape of the particles.

The output characteristics to this model is as; 1) Drag & lift coefficients. 2) Plastic Force [11]

## 1.6 Newtonian fluids:

Those fluids whose viscous stresses ascending due to flow at each point in linear way, are directly proportional to the rate of change of deformation.

Indeed, if the tensors which define the strain rate and the viscous stress are correlated through the constant tenor of viscosity which are not dependent on the velocity and the stress rate of fluid flowing.

For the account of the viscosity of the fluids, these are the modest models in mathematical form. Virtually, none of the real fluids act exactly as the Newtonian fluids but can be assumed as the Newtonian fluids for carrying out calculations under the normal conditions for most of the common gases and the liquids just like air and the water

## 1.7 Non-Newtonian fluids:

The fluid that does not trail the Newton's viscosity law. Typically, the viscosity of such fluids be contingent on the rate of shearing, where most of the fluids show the normal difference in the stress having non- shear depending viscosity. So many examples can be found in our daily lives including custard, ketchups, honey, blood, toothpaste, shampoo etc.

## 1.8 Shear Thickening fluids:

When the rate of shear is increased, fluid's viscosity also upsurges as the time passes, such fluids are known as the Shear thickening fluids (or dilatant fluids). Typical example is when corn starch is mixed in water, if stirring is firmly, its looks less viscous but if the mixing or stirring rate is increased it shows liquid with viscous effects.

## 1.9 Shear Thinning fluids:

These are reverse of shear thickening fluids and the viscosity of fluid decreases with time. These are also known as the pseudoplastics. Common example may include the blood in the human body because the flowing of the blood causes to reduce by raising the rate of shear strain.

## 1.10 Bingham Plastics:

Prior to flow these fluids entail finite yield stress & have linear relationship of shear strain with the shear stress. Examples include toothpaste, clay, mud used in drilling, chocolate etc.

## 1.11 Rheopectic Fluids:

For preserving continual rate of strain, these involve steady shear stress raising and rate of strain of such fluids are function of time is known as rheopectic fluids. Reverse case is known as thixotropic, in which fluid need reducing stress for steady rate of strain makeup, hence the with the passage of time, fluid thins out.

## 1.12 Fluid Power-Law:

It is used to define the attributes of non-Newtonian fluid. It is also known as the Ostwald~de~waele relationship, It can be written in mathematical form as:

$$\mu eff = \kappa \left(\frac{\partial u}{\partial y}\right)^{n-1}$$

Where,

μeff is the apparent viscosity and is given by Pascal-second

K is the index of consistency and is given by Pascal-second raise to power n,

∂u/∂y is gradient of velocity normal o the shear plane and is denoted in per second units,

& n is the flow behavior index and has no units.

Depending on the value of n, power law fluids are divided in three categories, among which,

If n is less than 1, it is said to be Pseudoplastic; if n is equal to 1, it is said to be Newtonian fluid and when the value of n is greater than 1, is Dilatant[12]

# Chapter 2

# Literature Analysis

## 2.1 Review of Literature:

It includes the discussion on various impacts on rate of accumulation. This chapter is mainly consisted of the literature regarding the eccentric annuli. Conveyance of cuttings proficiently is very stimulating while drilling the wells horizontally. Issues like bit wearing in prematurity, pipe-stuck, accumulation of cuttings also higher drag and torques can be caused because of poor cleaning of bore-holes. For the determination and solution of the problems like borehole cleaning was resolved through controlling by flowrate method, detect method for hole cleaning, chemical or mechanical cleaning method [13]. Drilling fluid is thrusted by mean of high pressure pumps in the drilling pipe and is departed through drill-bit afterwards mixture of formation cuttings and drilling fluid returns via annulus amongst inner pipe and the hole of bore which is elevated to surface level at the end [14, 15]. The exploration of well drilling has been lengthily scrutinized for the determination of flow and cutting characteristics. Rheological properties of drill-fluid have robust impact on cutting transportation, flowing through the annulus of wellbore [15]. The equations grounded on angular momentum and linear conservation, continuity, fluid flow characteristics. Newtonian and Non-Newtonian are two groups upon which fluids are segmented. The appearances of Newtonian fluids are being illustrated through the most lower molecular weighted materials like liquids of inorganic and organic material whereas, the belongings of Non-Newtonian fluids deviate from Newtonian fluids on vast scale. In certainty, most of the fluids depict Non-Newtonian comportments which includes toothpaste, ketchup, paint, shampoo, molten, blood, salt solutions and starch suspensions [16].

By using Third grade model of fluid, representation of temperature and flow has been offered, the thermodynamic investigation for non-Newtonian fluid which flows through the annular region, has also been carried out in previous studies [17]. For the betterment of production of food, crystals formation, bearing and pipes, microchannel, heat transfer on convection basis has been nowadays fascinated because of

applications [18]. Eccentricity and buoyancy forces can be used for the determination as well as description of heat and flow in mixed convection heat transfer cases having radius ration constant [19] .

For the transportation of cuttings, many numerical and experimental studies have been described which consists of rheological properties, eccentricity of drilling pipe, inclination of wellbore, diameter and rotational speed of inner cylinder of drill-pipe. Regardless of drilling pipe rotation, most of the experimental studies have been made on cuttings conveyance but study on drilling pipe rotation is limited in the literature on numerical validation [20].

Upon the experimental evaluation, the transportation of particles in strayed wellbores was studied and found properties based on lifting of cuttings through thin hole annulus by using liquid solid mixture [21] [22]. By measurement of pressure loss and the volumetric concentration of constituents, flowing properties of mixture in the closed loop was also estimated in the test section. In the geometry of annulus, these results played an important role for the explanation of phenomenon of transportation and consequences of solids in the mixture and drill pipe rotation in well drilling. Pressure drop and cuttings fractional volume are substantially affected through inner cylinder rotation, at medium or the lower flowing rates, however after approaching the critical speed, no such effect on the flowrates could be found [21].

Mostly Non-Newtonian fluids with high yield stress and viscosity with low effectiveness are used due to operative holding capacity and binding ability of the solids in the mixture throughout the stationary time phase. Annulus mostly becomes eccentric in horizontal drilling wells and due to the reason, that in the narrowest gaps, the velocity is minimal hence the accumulation is prone in the such plane. As in the turbulent flows, the probability of such effect is lower therefore the present results illustrate some important properties such as rotation of shaft, viscosity, flowing geometry, Reynolds number [23].

Non-Newtonian eccentrically flowing fluids through the annulus with unrotated and rotated ones, and summary of this report is accessible in table (2). In annuli non-Newtonian fluid velocity typescripts could be nearly correlated to CMC aqueous solution, which was used for drill mud modelling & three aqueous solutions including CMC solution, gum of xanthan and combination of CMC & laponite, which are used

by [24]. The size of annulus was taken greater, accomplished by past investigators with constant ratio of the diameter & contract amongst results of the polymer solution, found upright. The drag reduction was found in turbulent flow and this proves the identical resistance to that Newtonian flow regime. It is usually noted that tangential velocity decays swiftly through rotating inner cylinder while much slighter decay is noted in maximum in the core region of annuli. With increase in Reynold number swirl decreases. Additional resisted & even axial flow are obtained by rotation. Experimental studies discovered that rotation enhances the concentrations of whole turbulence, specifically the crossflow components with both fluids, that the drag decrease effect associated with the shear-thinning non-Newtonian fluid was larger with rotation, as was the difference in turbulence intensities between the Newtonian and non- Newtonian fluids for the identical Reynolds number [25]. Newtonian and non-Newtonian fluids flow experimental studies in eccentric annuli with inner cylinder rotation has not been done and the recent studies reveals the effects of rotated center body with various Reynolds no. & flow assemblies. For quantities the value eccentricity was used as 0.5.

By striking of an axial flow creates a differential. The axial pressure gradient swings the appearance of the Taylor vortices towards rotational rate up to greater extent due to rotational inner wall of the annulus [26]. Newtonian fluid flows with cuttings or non-Newtonian single-phase flows have been used for preceding researches. Annulus could be comprised of laminar as well as completely turbulent (i.e. spacer fluid of low viscosity, chemical washing fluid) in a single fluid [27]. The effect of non-Newtonian characteristics of drilling fluid and rotation of inner pipe on cuttings transport performance were studied by few researchers. kinetic theory of granular flow in combination with Eulerian-Eulerian two-fluid models to predict the effect of drilling fluid rheological properties, annular velocity, well inclination, drill pipe rotation, ROP and cuttings size on cuttings transport and pressure drop in the annulus were used to study fluid-cuttings flow in annular space. Basis of kinetic theory of granular flow depends upon similarities between the flow of a granular material with or without an interstitial gas and the molecules of a gas [28].

By using the horizontal annulus along with the limited restrictions, experimental arrangement was conducted to evaluate the pressure drop data, operational conditions, geometrical impacts and viscosity effects of that fluid were also measured for the

calculation. Velocities were calculated by means of CFD due to some experimental restrains [29].

Extensive variety of detailed experimental data has also been given in literature or flow environments in pneumatic transport [30]. The Modelling of rheologic properties of particles including dynamic viscosity, bulk viscosity and particle pressure due to the collisional interactions of particles can be done as the function of granular temperature. Debate on kinetic theory of granular flow and its application for studying fluid-cuttings two-phase flows considering non-Newtonian fluid properties restitution was given by . Modeling of the collisional and kinetic transport mechanisms for the momentum and fluctuating kinetic energy of cuttings results in a description of the momentum transport properties as a function of the granular temperature. The drilling fluid phase and the cuttings phase is strongly coupled by the interaction forces amongst them. Following assumption are assumed that (1) the liquid phase has constant density and non-Newtonian fluid with Power-low model, (2) the cutting is assumed as spheres with a mean particle diameter and density, and (3) no interfacial mass transfer taking place between two phases. The flowing of granular material of a finite mass through the plane of inclination at the horizontal surface, also problem of dam-break and flowing behavior has also been studied in the literature [31].

In this research work, investigational data of annular flow in the eccentric annulus with unlike flowrates and rotational speed, have been measured using numerical techniques and noted the behavior of flow in the narrow gap by rotating inner pipe of annuli. Simulated comportments have also been compared with the experimental data and found similar trend for the axial and tangential mean velocities.

## 2.2 Objective

In this study, Computational Fluid Dynamics (CFD) grounded simulation has been achieved for the accumulation problem faced during drilling of oil and gas wells. After the incorporation of required input data to the software, simulation analysis is performed, and results are obtained. Objectives included in this study comprises of an eccentric annulus model design using ANSYS Fluent Software. The study also includes the effect of rotational speed in CFD to overcome accumulation problem during drilling well and validation of this model with the literature work.

# Chapter 3

# Mathematical Modelling Based on CFD

## 3.1 Background:

Fluid dynamics is the branch of physics, which describes the flow characteristics of fluid. It is further subdivided in many branches among which CFD (Computational Fluid Dynamics) is the field which solves the problems by utilizing the data structure and the numerical analysis, which are concerned with the flow of the fluid. To study the flow behavior in the annulus for drill fluid and cuttings, Eulerian-Eulerian two-phase model for flow was used. Cuttings are taken as a band in the two-fluid model, as in the phase of liquid. Every phase is categorized through its equation of motion for conservation in the respective two interpenetrating solid and liquid phases. Kinetic theory of granular flow is used for the collision and kinetic momentum transfer for the modelling of cuttings, where the relation among the two phases are illustrated in the form of additional source terms supplemented to the equations of conservation. The inelasticity is considered by means of Compensation coefficient when the cuttings kinetic energy is consumed during the impacts among the sets of particles. Kinetic transport and collisional momentum and instable cuttings kinetic energy is modelled through the granular temperature $\varrho_s = [c]^2/3$, where [c] is the cuttings instable velocity. The cuttings and drilling fluid is sturdily bonded through the forces of interaction among them. We propose that (1) Power-law model is used for liquid phase in Non-Newtonian incompressible fluids, (2) The cuttings are mean density and diameter of particle in the form of spheres and (3) Among the two-phases, no mass transfer on interfacial basis befalls.

## 3.2 Methodology

### 3.2.1 Preprocessing

The preprocessing is consisted of the following steps involved:

- For defining the physical geometry & the problem's boundary & the volume of fluid, CAD is used which stands for Computer aided design.

- So, the engaged volume of the fluid alienated and hooked with the discrete cells of the geometry which is known as the mesh or grid. Such grid can be pyramidal, symmetric or asymmetric, uniform or not, tetrahedral, structured or not structured cells of the mesh.
- The grid is described through the radiation, molecular conservation equation, motion of the fluid.
- Classification of Boundary conditions is also stimulated.

### 3.2.2 Processing

Until the convergence and calculation of simulations are achieved by using the differential equations, simulations are administered and hence transient or steady state conditions are obtained.

### 3.2.3 Post-processing

By the envisioning and investigation of the solution, post-processing is obtained lastly.

## 3.3 Environment of Simulation

### 3.3.1 ICEM 18

Nowadays many software has been arrived for the designing of geometries including ICEM, AutoCAD, IGES, Gambit and much more. The software used in this study is ICEM which was found easy and user friendly with numerous functions that are missing in rest of CAD software. By means of vertices, geometry with 3dimensional attributes was created. Faces are created through the using the edges, which are obtained through the linked vertices. Eventually, unistructural meshes are generated which comprises of the categorized boundary conditions mentioned at the edges where the faces are categorized with the various zones. Graphical user interface of ICEM can be given as:

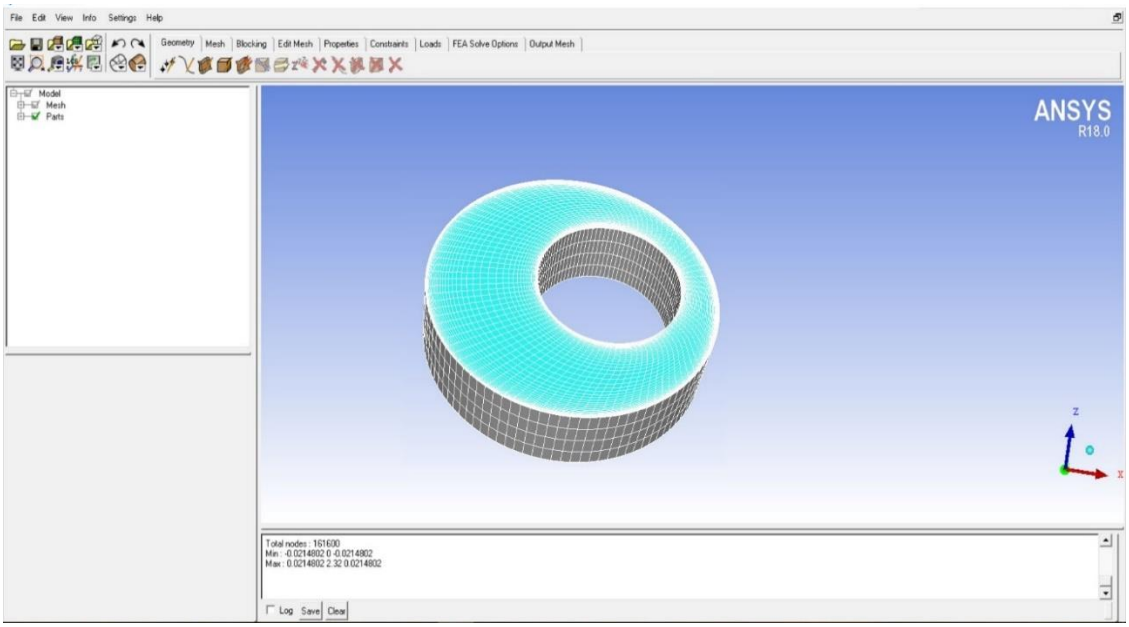


Figure 3 ICEM GUI

### 3.3.2 Ansys Fluent

Furthermore, geometry was imported to Ansys Fluent through ICEM. Method used in this study is comprised of Control volume method. Quality of the grid has been evaluated through Fluent. Boundary, periodic and zonal conditions were than defined stepwise. Scale was selected as mm.

Finite length eccentric annulus has been used in this study as the computational domain. Deprived of crashes or pore channels, wellbore wall is firm. Over the whole simulated length, no tool joint is used inside the axial length of the annuli with a solitary drilling pipe. At the itemized speed of rotation, inner pipe rotates about self-axis. Figure (6) depicts the computational mesh and geometry structure of annular space. 8-5/8-inch casing outer diameter (inside diameter of 08 inches to be attained after subtracting wall thickness), outside diameter of 04inches of drill pipe opted. Boundary condition values and other parameters illustrated in table (2) originated from experimental values, [23]. At the exit of the annulus, pressure boundary conditions are set as atmospheric. At 1atm, pressure has been set at the outlet. For the modelling of granular temperature and velocity, no-slip boundary conditions were used. Particle compensation and secularity, values of 0.9 to 0.1 to be assumed as the coefficient values. Sliding mesh in the annulus was applied to simulate the impact of drilling pipe rotation on transport of cuttings. Annulus was categorized as outer and

inner flowing zones. Inner flow zone is rotating at the similar rotational speed as of drilling pipe and outer zone is stationary. On every cell, finite volume approach was discretized as the governing equations for the annulus. Pressure discretization scheme has been followed using SIMPLE routine in the calculations. Second order implicit for integration of time, for solving momentum equations and for the volume fraction interpolation, QUICK routine was opted for improved acclimatization of hexahedral meshes in simulation. Above mentioned simulation stratagem was passed through CFD. Convergence time step was opted 0.00001 sec. Several values of time average were attained from simulation and through hexahedral meshes, establishing the structured mesh, three-dimensional meshes were gathered. Computational Mesh used in this model is shown in figure (4). Grid size was consisted of 20,000 cells, 60400 faces and 25500 Nodes.

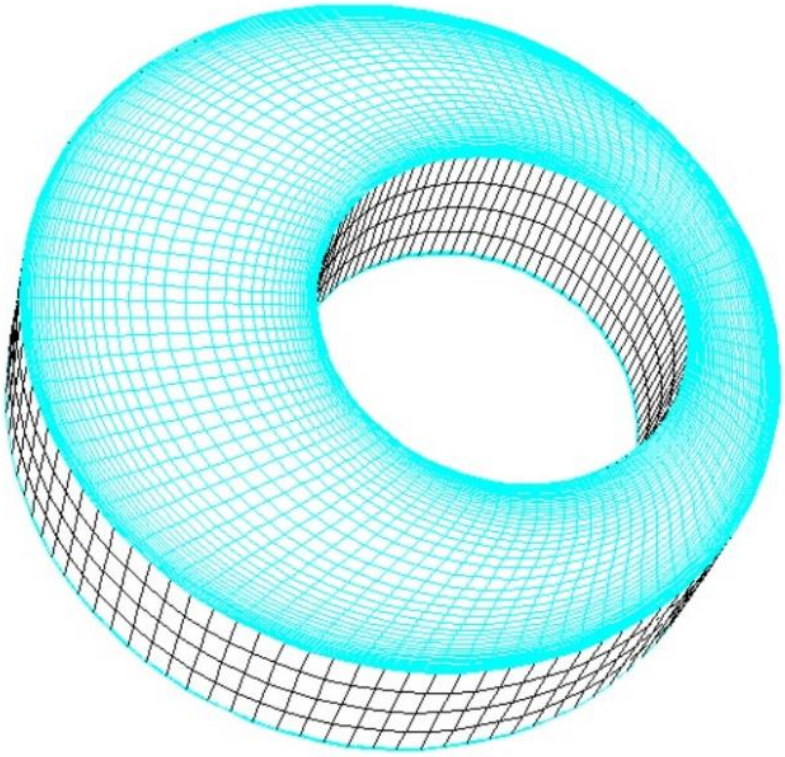

Figure 4 Computational Mesh and Geometry domain

## 3.4 Meshing

While simulating in ANSYS ICEM, the result of the problem be contingent sturdily on the quality of mesh. For the solution of the problem, mesh should be evocative. The meshing of the computational domain is done in ANSYS ICEM CFD. ANSYS ICEM CFD is a sophisticated tool for mesh creation.

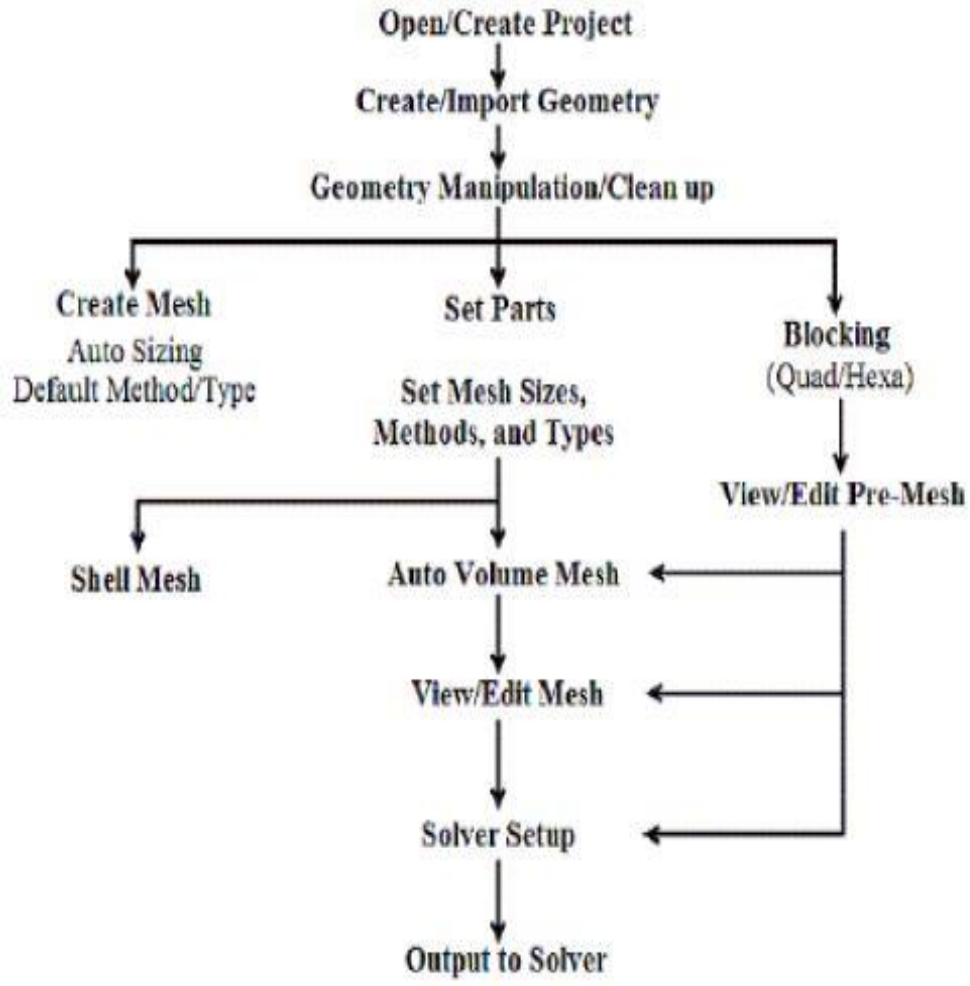


## 3.5 Criteria of convergence:

The commonly used absolute convergence criteria for the residuals of continuity, x-velocity, y-velocity, epsilon and species equation is .001 while the convergence criteria are 1e-04 for the simulation.

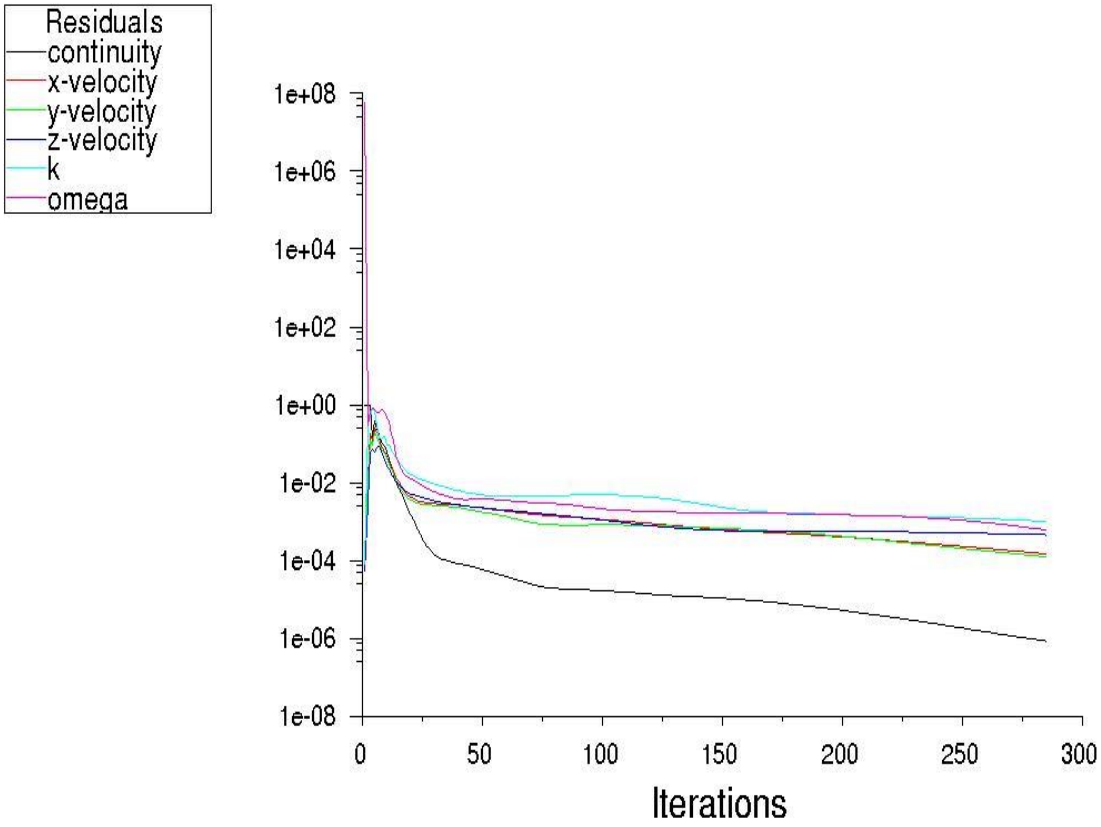


Figure 5 Convergence criteria

## 3.6 Independence of Mesh

Analysis in CFD for any solution purely depends on the mesh elements and the size. The purpose of mesh individuality learning is to ensure that at what number of elements the solution becomes sovereign from the element size of the mesh. Following table consists of different characteristics in Table 1.

Table 1 Mesh Properties

| **Mesh Properties** | **Values** |
|---|---|
| Orthogonal quality (Minimum) | 0.1326 |
| Ortho Skew (Maximum) | 0.8674 |
| Aspect Ratio (Maximum) | 172.94 |
| No of Nodes | 25,500 |

| | |
|---|---|
| No of cells | 20,000 |
| No of faces | 60,400 |
| Minimum Volume ($m^3$) | 2.4553 |
| Maximum Volume ($m^3$) | 2.6120 |
| Total Volume ($m^3$) | 9607 |
| Minimum Face area ($m^2$) | $9.8208 \times 10^{-3}$ |
| Maximum Face area ($m^2$) | 3.1961 |

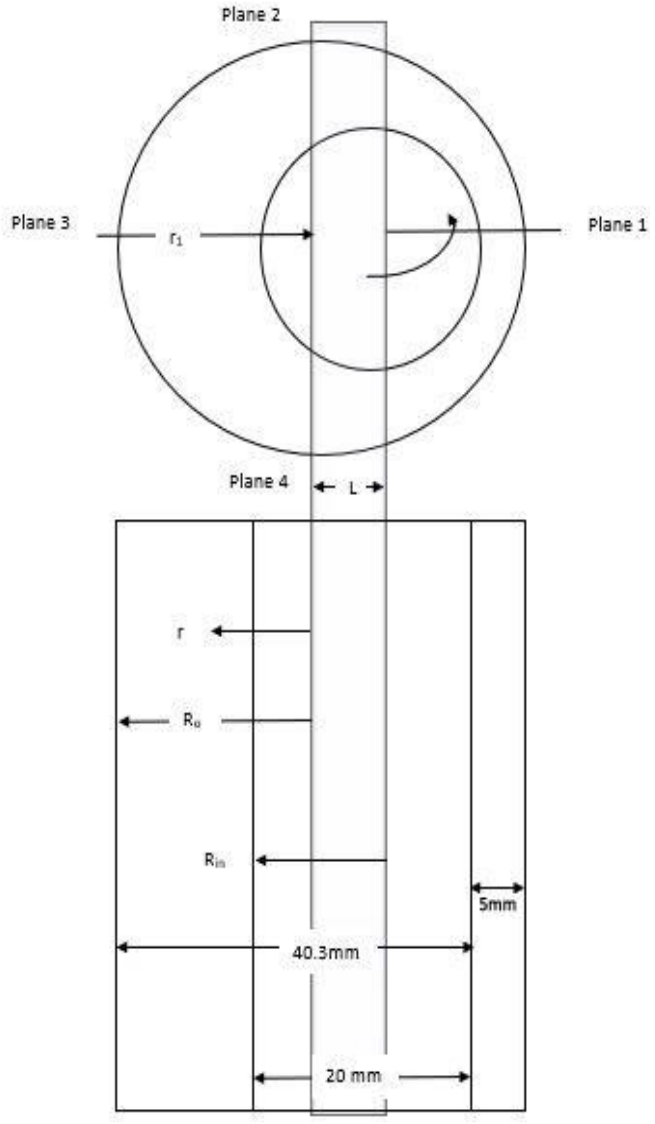


Figure 6 Schematic of eccentric annulus

## 3.7 Mathematical model:

To study the flow behavior in the annulus for drill fluid and cuttings, Eulerian-Eulerian two-phase model for flow was used. Cuttings are taken as a band in the two-fluid model, as in the phase of liquid. Every phase is categorized through its equation of motion for conservation in the respective two interpenetrating solid and liquid phases. Kinetic theory of granular flow is used for the collision and kinetic momentum transfer for the modelling of cuttings, where the relation among the two phases are illustrated in the form of additional source terms supplemented to the equations of conservation. The inelasticity is considered by means of Compensation coefficient when the cuttings kinetic energy is consumed during the impacts among the sets of particles. Kinetic transport and collisional momentum and instable cuttings kinetic energy is modelled through the granular temperature $\varrho_s = [c]^2/3$, where [c] is the cuttings instable velocity. The cuttings and drilling fluid is sturdily bonded through the forces of interaction among them. We propose that (1) Power-law model is used for liquid phase in Non- Newtonian incompressible fluids, (2) The cuttings are mean density and diameter of particle in the form of spheres and (3) Among the two-phases, no mass transfer on interfacial basis befalls.

### 3.7.1 Drilling liquid conservation equations:

The equation of continuity is illustrated as:

$$\frac{\partial}{\partial t}[\varepsilon_1\rho_1] + \cdot\,[\varepsilon_1\rho_1 v_1] = 0 \qquad (1)$$

Where, $v_1$ is velocity vector for liquid, $\boldsymbol{\rho_l}$ is density of liquid, and $\boldsymbol{\varepsilon l}$ is liquid phase volume concentration. The equation for momentum conservation is illustrated as:

$$\frac{\partial}{\partial t}[\varepsilon_1\rho_1 v_1] + \nabla\cdot[\varepsilon_1\rho_1 v_1] = \varepsilon_1\nabla\cdot\tau_1 + \varepsilon_1\rho_1 g - \varepsilon_1\nabla p - \beta[v_1 - v_s] \qquad (2)$$

Where, $\boldsymbol{\beta}$is coefficient of drag among the cuttings and the fluid, $\boldsymbol{\tau_1}$ is liquid stress tensor and **g** is acceleration due to gravity.

Power law equation for fluid can be illustrated as:

$$\tau_1 = \eta[\mathrm{D}].\mathrm{D} \tag{3}$$

where **η** is the apparent viscosity and is fluids shear stress and **D** is tensor of Rate of deformation and is defined as:

$$\mathrm{D} = \left[\frac{\partial v_{1j}}{\partial \mathrm{x}_i} + \frac{\partial v_{1i}}{\partial \mathrm{x}_i}\right] \tag{4}$$

Generally, **η** is tensor of Rate of deformation and is function for all three of variants and shearing rate function

$$\eta = \mathrm{K}\left[\sqrt{\frac{1}{2}D{:}D}\right]^{n-1} \tag{5}$$

where, n is index of power-law and K is consistency factor. If n becomes equal to 01, it's a Newtonian fluid where the fluid rheological characteristics segregated in two portions. If n is greater than 1 than its shear thickening fluid and if n is less than 1 than its shear thinning fluid.

In this work, drilling fluid flow through annulus is whichever low Reynolds number turbulent or laminar flow. Modifications for low Reynolds number for K- ω model have been anticipated by Wilcox. Shear stress transport K- ω model was casted for drilling fluid in case of turbulent viscosity by Menter. By using the following transport equations, specific dissipation rate **ω** and **K,** the kinetic energy can be attained:

$$\frac{\partial}{\partial \mathrm{t}}[\rho_m\, k] + \frac{\partial}{\partial x_i}[\rho_m\, k\, v_m] = \frac{\partial}{\partial x_j}\left[\Gamma_k \frac{\partial \mathrm{k}}{\partial x_j}\right] + G_k^* - \mathrm{Y}_k \tag{6}$$

$$\frac{\partial}{\partial \mathrm{t}}[\rho_m\, \omega] + \frac{\partial}{\partial x_i}[\rho_m\, \omega\, v_m] = \frac{\partial}{\partial x_j}\left[\Gamma_\omega \frac{\partial \omega}{\partial x_j}\right] + G_\omega - \mathrm{Y}_\omega + \mathrm{D}_\omega \tag{7}$$

Where, $G_\omega$ is generation of ω, $G^*_k$ signifies turbulence kinetic energy turbulence. Effective diffusivity of k and ω is given by $\Gamma_k$ and $\Gamma_\omega$ respectively. Dissipation due to turbulence of ω an k is $Y_\omega$ and $Y_k$ respectively. Cross diffusion is defined by $D_\omega$

### 3.7.2 Coefficient of momentum transfer interphase:

According to the correlation of Gidaspow-Huilin, the drag forces among the cuttings and the drill fluid are premeditated. The model of Gidaspow-Huilin is amalgamation of Ergun- equation and the model of Wen and Yu defined by [25, 32].

$$\beta = \varphi\beta\, Ergun + (1-\varphi)\beta \text{WenandYu} \tag{8}$$

$$\varphi = \frac{1}{2} + \frac{\arctan\{263.5(\varepsilon s - 0.2)\text{Error! Bookmark not defined.}}{\pi} \tag{9}$$

$$\beta\, Ergun = \frac{\varepsilon_s^2 \mu_1}{\varepsilon_1\, d_s^2} + 1.75\frac{\varepsilon s \rho 1}{ds}\,[\nu_1 - \nu_s] \tag{10}$$

$$\beta_{\text{WenandYu}} = 3\frac{C_d \varepsilon_1 \varepsilon_S \rho_1 [\nu_1 - \nu_s]}{4ds}\varepsilon_1 - 2.65 \tag{11}$$

Where $C_d$ is the drag coefficient and is defined as:

$$C_d = \frac{24}{Re_s}[1 + 0.15Re_s^{0.687}], Re_s \leq 1000 \tag{12}$$

$$C_d = 0.44, Re_s > 1000 \tag{13}$$

Where Cuttings phase Reynolds number can be illustrated as:

$$Re_s = \frac{\varepsilon_1 \rho_1 d_s [\nu_1 - \nu_s]}{\mu_1} \tag{14}$$

### 3.7.3 ANSYS CFX k-omega Model:

For low Reynolds number calculations for near wall treatment, k-ω formulation is very helpful. The model is more precise and vigorous because it does not contain complex nonlinear functions for the requirement of K-ω model. From a low Reynolds number to wall function formulation, smooth shift is obtained through it.

It is supposed in the K-ω model that, turbulent frequency and turbulent kinetic energy is related with turbulence viscosity, which is:

$$\mu_t = \rho\frac{k}{\omega} \tag{15}$$

### 3.7.4 Wilcox k-0mega Model

Wilcox developed the k-ω model for this formulation, which solves two equations of transport, one for the turbulence frequency (ω) and other for the turbulent kinetic energy (k). From eddy-viscosity concept, stress tensor is calculated.

ω-equation:

$$\frac{\partial[\rho\omega]}{\partial t}+\frac{\partial}{\partial x_j}[\rho U j\omega]=\frac{\partial}{\partial x_j}\left[\left(\mu+\frac{\mu t}{\sigma\omega}\right)\frac{\partial\omega}{\partial x_j}\right]+\alpha\frac{\omega}{k}Pk-\beta\rho\omega 2+P\omega b \quad (16)$$

K-equation:

$$\frac{\partial[\rho k]}{\partial t}+\frac{\partial}{\partial x_j}[\rho U j k]=\frac{\partial}{\partial x_j}\left[\left(\mu+\frac{\mu t}{\sigma k}\right)\frac{\partial k}{\partial x_j}\right]+Pk-\beta'\rho k\omega+Pkb \quad (17)$$

By Navier-Stokes method, velocity vector(U), density(ρ) and other independent variables are taken as known measures. In above equation, $P_k$ is turbulence production rate and can be computed from k-ε model, where the constants of model are as under:

β'= 0.09; α=5/9; β=0.075; $\sigma_k$=2; $\sigma_\omega$=2

Computation of unknown Reynolds stress tensor $(\rho\overline{u_i u_j})$

$$-\rho\overline{u_i u_j}=\mu t\left[\frac{\partial U_i}{\partial X_j}+\frac{\partial U_j}{\partial X_i}\right]-\frac{2}{3}\delta ij\left[\rho k+\mu t\frac{\partial U k}{\partial x k}\right] \quad (18)$$

Table 2 Simulations input parameters summary

| **Notation** | | **Units** | **Simulation Value** |
|---|---|---|---|
| $d_h$ | hydraulic diameter ($D_o$-$D_{in}$) | mm | 20.3 |
| $D_o$ | outer pipe diameter | mm | 40.3 |
| $D_{in}$ | inner cylinder diameter | mm | 20 |
| Re | bulk flow Reynolds number ($U_b$ $d_h$/ v) | | 1140, 9300, 1150, 9300 |
| Rs | Rossby number (2 $U_b$/ω $R_{in}$) | | 0.0, 3.4, 17.35 |
| E | eccentricity {L/(Ro-Rin)} | | 0.5 |
| $R_o$ | outer pipe radius | mm | 20.15 |
| $R_{in}$ | Inner cylinder radius | mm | 10 |
| $U_b$ | Bulk velocity | $m.sec^{-1}$ | 0.56, 2.76, 0.54, 2.72 |
| $G_m$ | Mass flow rate | $Kg.sec^{-1}$ | 0.54,2.61,0.52,2.61 |
| V | Volumetric flowrate, X $10^{-3}$ | $m^3.sec^{-1}$ | 0.54,2.61,0.52,2.61 |
| $\omega_d$ | rotational speed of drill pipe | Rpm | 0.0,300 |
| P | Density of fluid | $Kg.m^{-3}$ | 1000 |
| $\mu_w$ | Effective viscosity, X $10^{-3}$ | $Kg.m^{-1}.s^{-1}$ | 10.0. 6.0, 9.5, 6.0 |

# Chapter 4

# Result and Discussion

## 4.1 Computational model validation

For the validation of simulations, single-phase drilling fluid in an eccentric annulus was achieved in contrast with experimental work. Primarily, annulus having eccentricity of 0.5 and inner cylinder rotating at the speed of 300 rpm was taken as non-Newtonian single-phase fluid. 0.2% CMC aqueous solution was used as the non-Newtonian fluid. By inserting the viscometric figures using power-law fluid, power-law consistency, was given as 0.044 $Pa.s^n$, power-law index 0.75, shear stress $\tau$ to shear rate $\Upsilon$ is given by $\tau = 0.044\ \Upsilon^{0.75}$.

Flow of power law fluid through the eccentric annulus, in contrast of premeditated data and the results obtained from simulations in narrow and wide gaps can be shown in the figures (10,11,12) & figures (19,20,21) respectively. Tangential and axial velocities in dimensionless form were plotted against the dimensionless length from inner cylinder's outer wall (Li/Gi) and prepared the fitted curves among dimensionless quantities. Li represents the inner cylinder's outer wall radial length and Gi represents the narrow or wide gap corresponding to the eccentric annulus. By relating the experimental verses simulated data, the comparison is practical and depicting the reasonable results of tangential and axial velocities obtained from simulation and found that the average errors were minimal corresponding to tangential and axial simulated velocities. Justification was permitted based on experimental and simulated work on the eccentric annulus with rotational drilling pipe and having single-phase non-Newtonian flow regime.

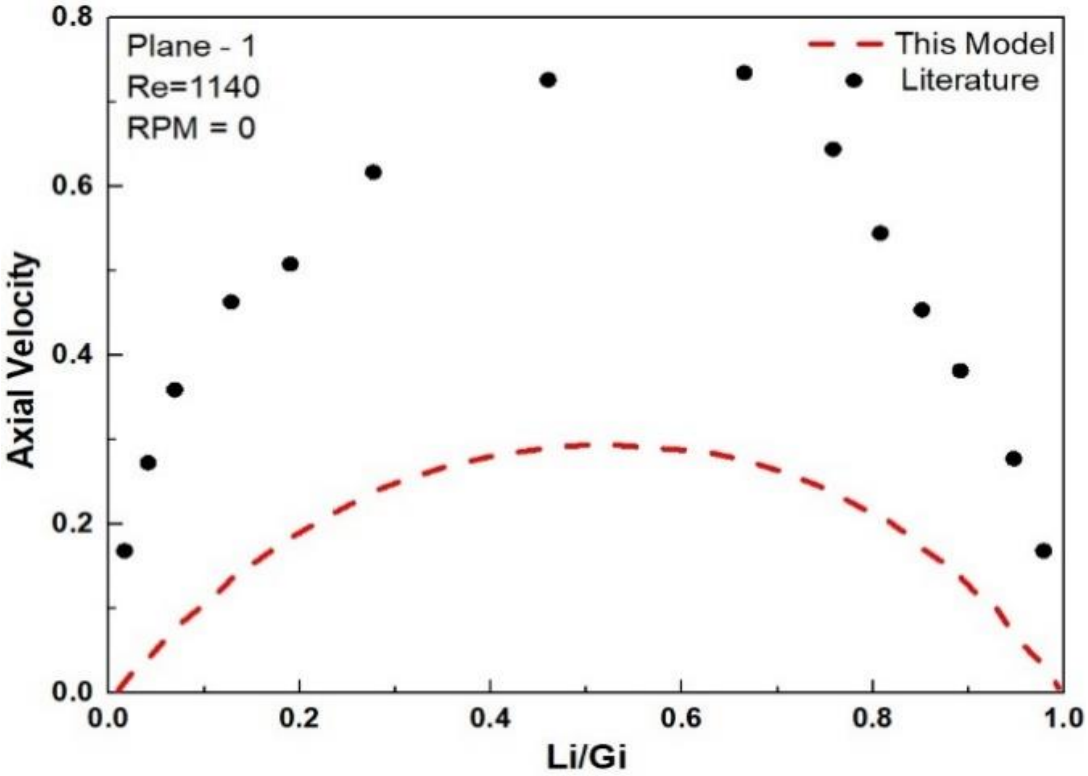


Figure 7 Axial mean velocities at plane-1; Re1140; RPM:0

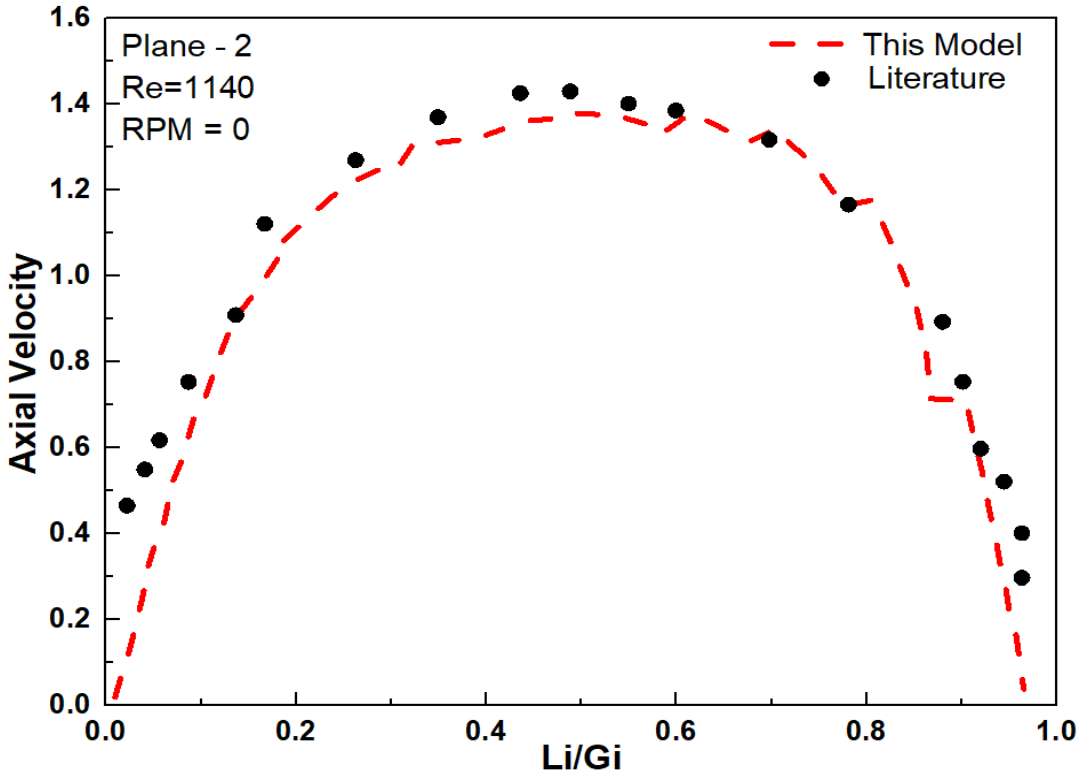


Figure 8 Axial mean velocities at plane-2; Re1140; RPM:0

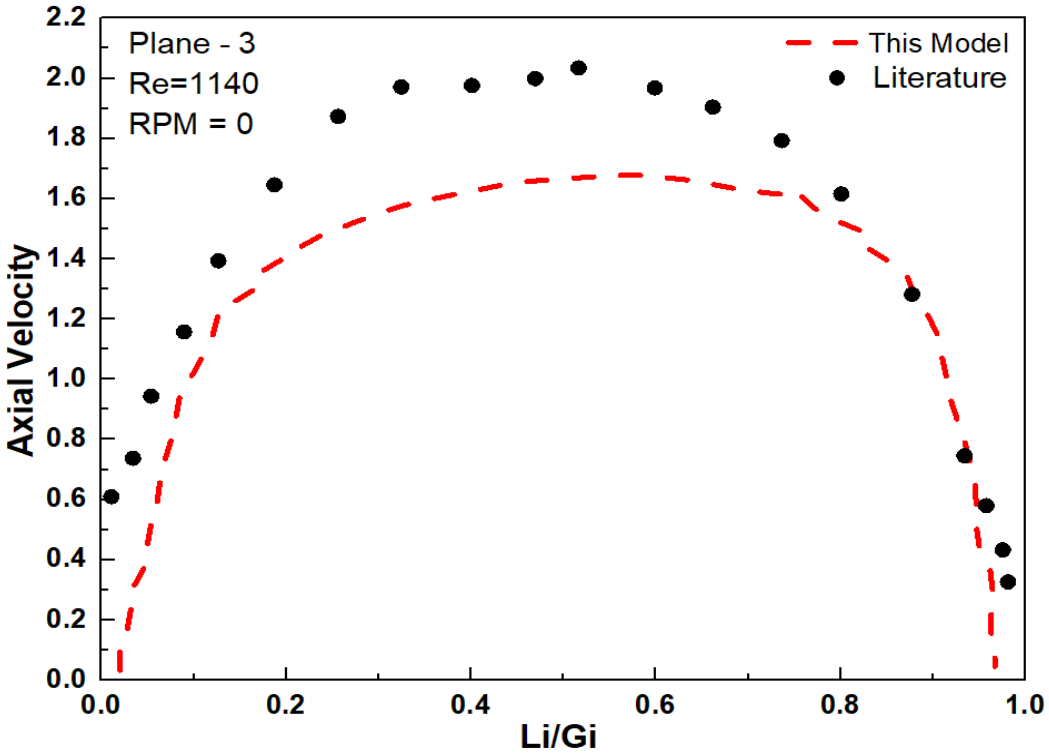


Figure 9 Axial mean velocities at plane-3; Re1140; RPM:0

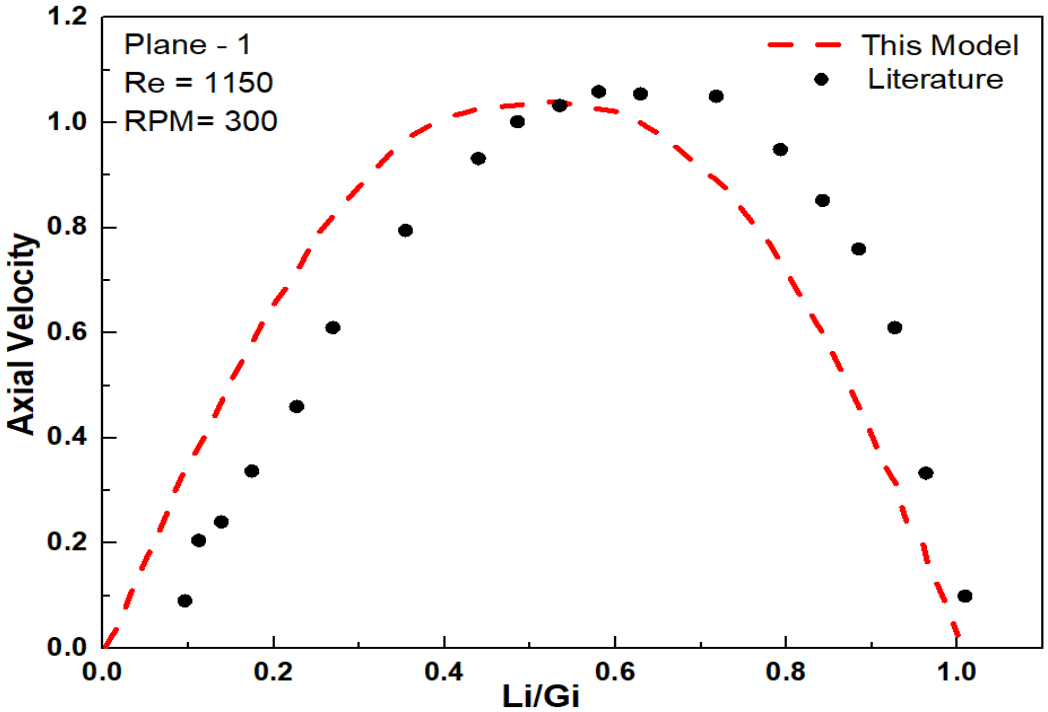


Figure 10 Axial mean velocities at plane-1; Re1150; RPM:300

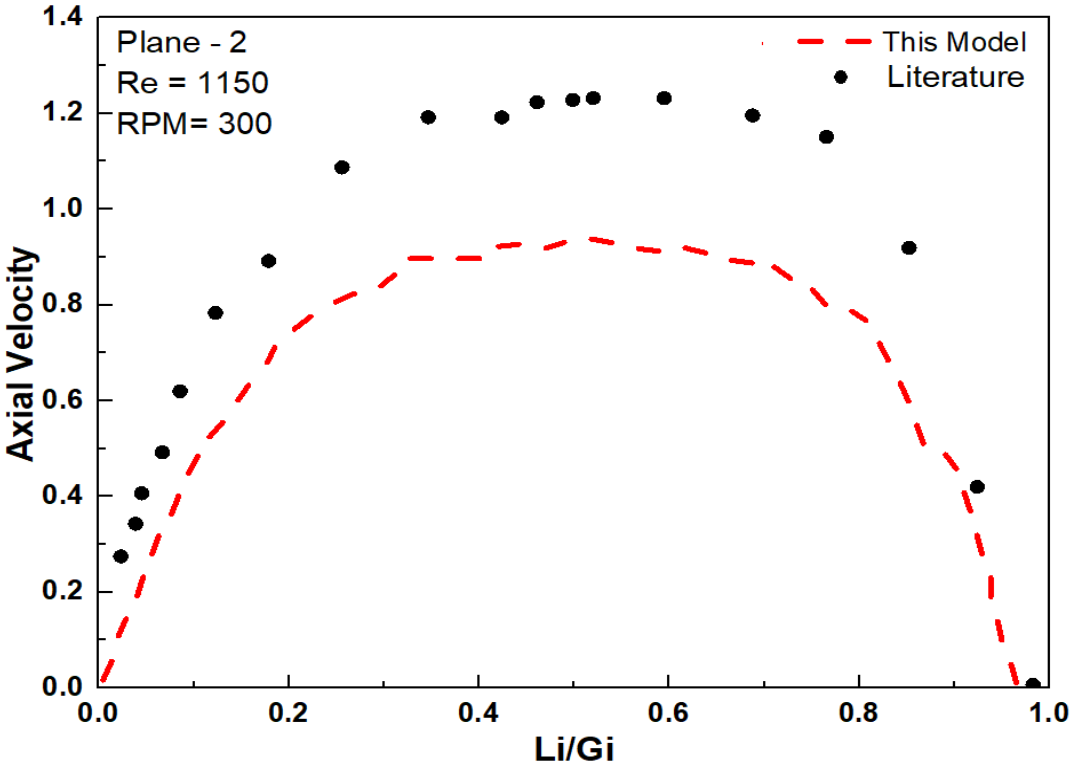

Figure 11 Axial mean velocities at plane-2; Re1150; RPM:300

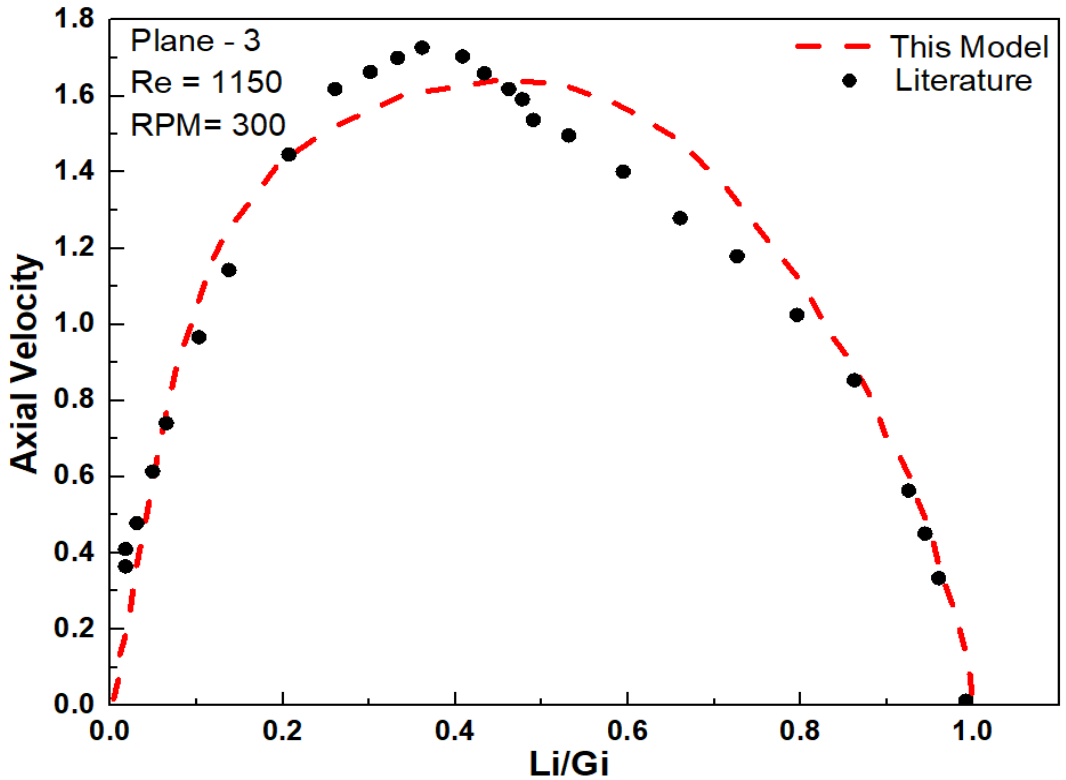

Figure 12 Axial mean velocities at plane-3; Re1150; RPM:300

## 4.2 Rotational flow Effect on non-Newtonian fluid

Along with the axial results related with the non-rotating flow, the mean velocities of 0.2% CMC solution at Rossby numbers of 3.4 and Reynolds number of 1150 are illustrated in figures (10,11,12), in which axial velocities at all 03 planes can be shown. There are overall 04 planes considered as shown in figure (6) and the whole simulation results are relied on it. Figures (7,8,9) & Figures (10,11,12) represent the axial mean velocities of all 03 planes for both 1140 and 1150 Reynolds number with 0 rpm and 300 rpm respectively. The effect of rotation on the axial flow in experimental results with respect to the simulations were almost similar where the results in non-rotational flow comparatively in plane -1 were in the extended array. Axial velocities in plane-2 were almost alike for experimental and this model. The difference among the wide and narrow gap velocities was found to be lower with the rotation and high without rotation. The alteration through the rotation was apparent in the axial mean velocities, the maximum velocity is transferred in the direction of outer wall, chiefly in plane-3 and the axial profile in the core region is smooth in plane-2. Counter-rotational flow was observed due to tangential mean velocities laterally through the outer pipe in plane 2 and 3, which was triggered because of radial adverse pressure gradient in the cylinder's outer wall. It has been suggested that reattachment from the outer drill pipe among planes 4 and 1 and parting between 1 and 2.

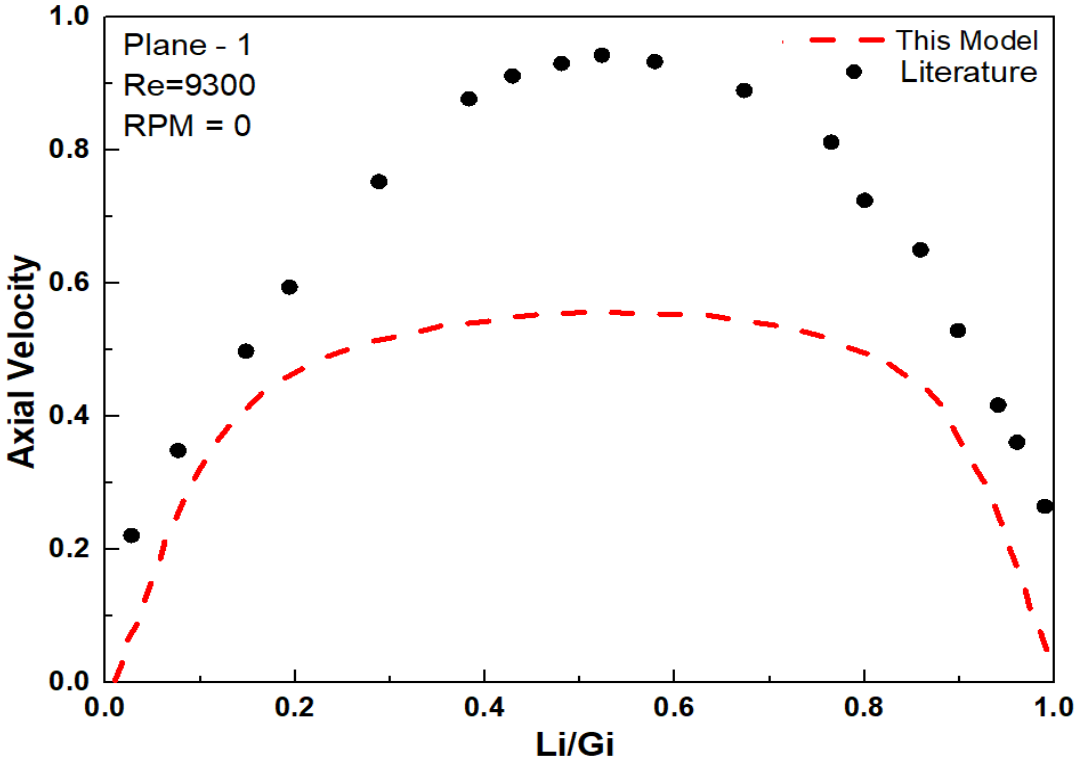


Figure 13 Axial mean velocities at plane-1; Re9300; RPM: 0

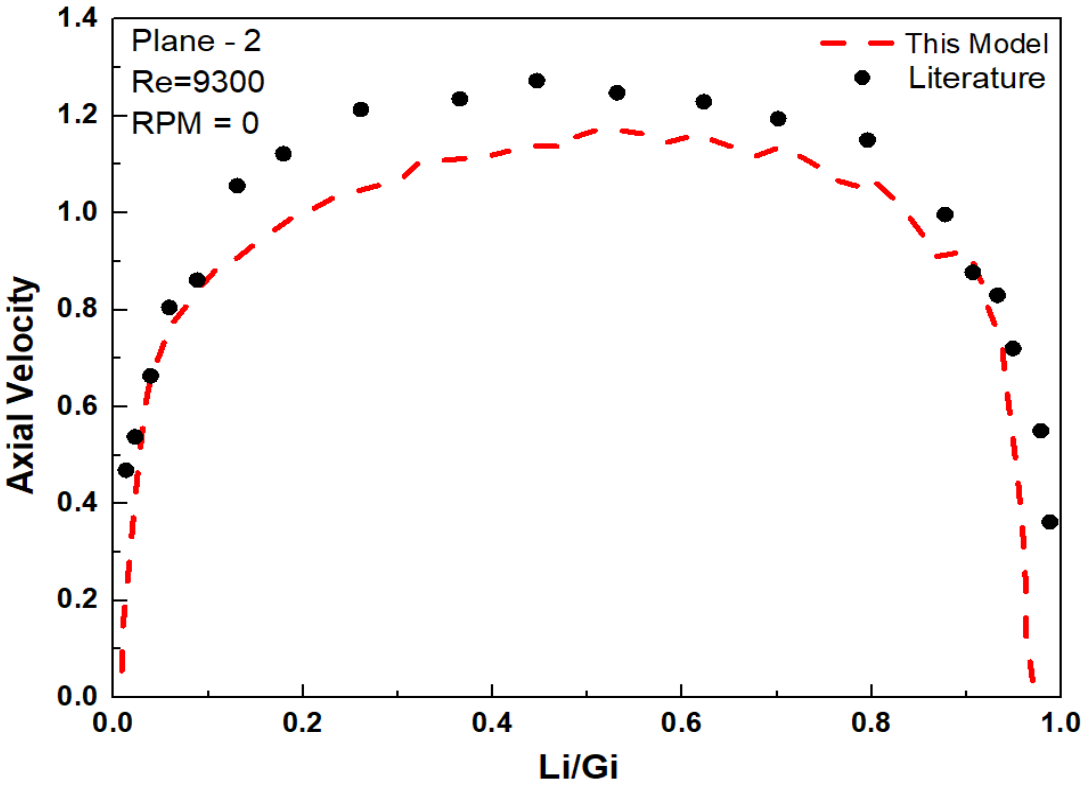


Figure 14 Axial mean velocities at plane-2; Re9300; RPM: 0

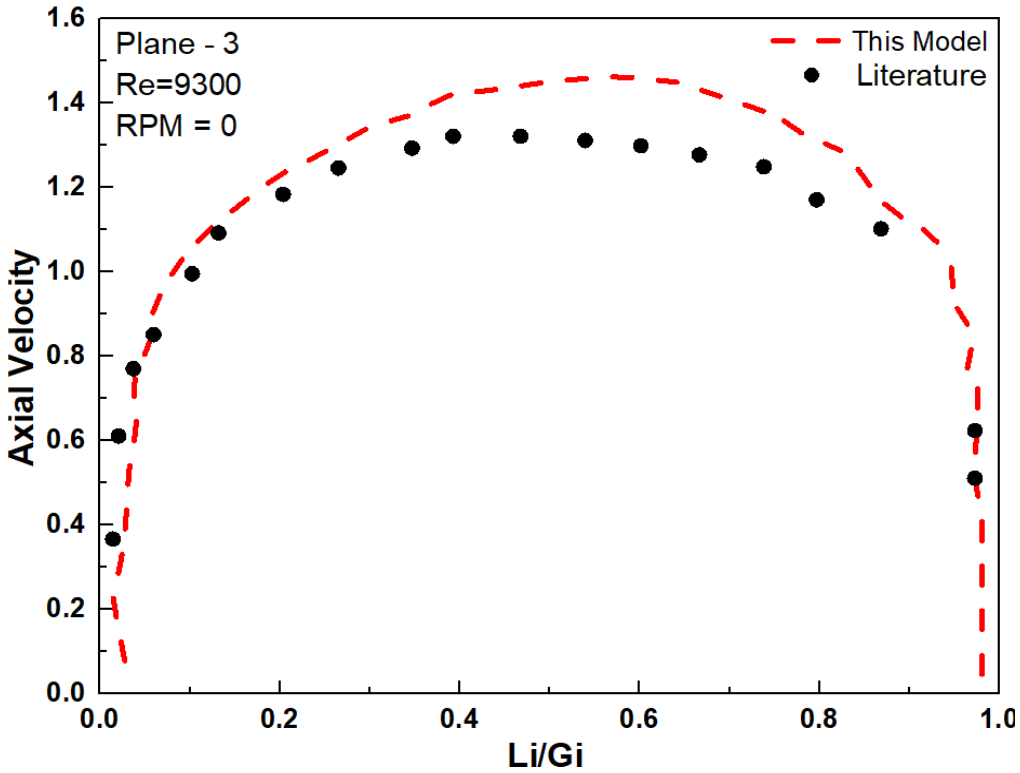


Figure 15 Axial mean velocities at plane-3; Re9200; RPM: 0

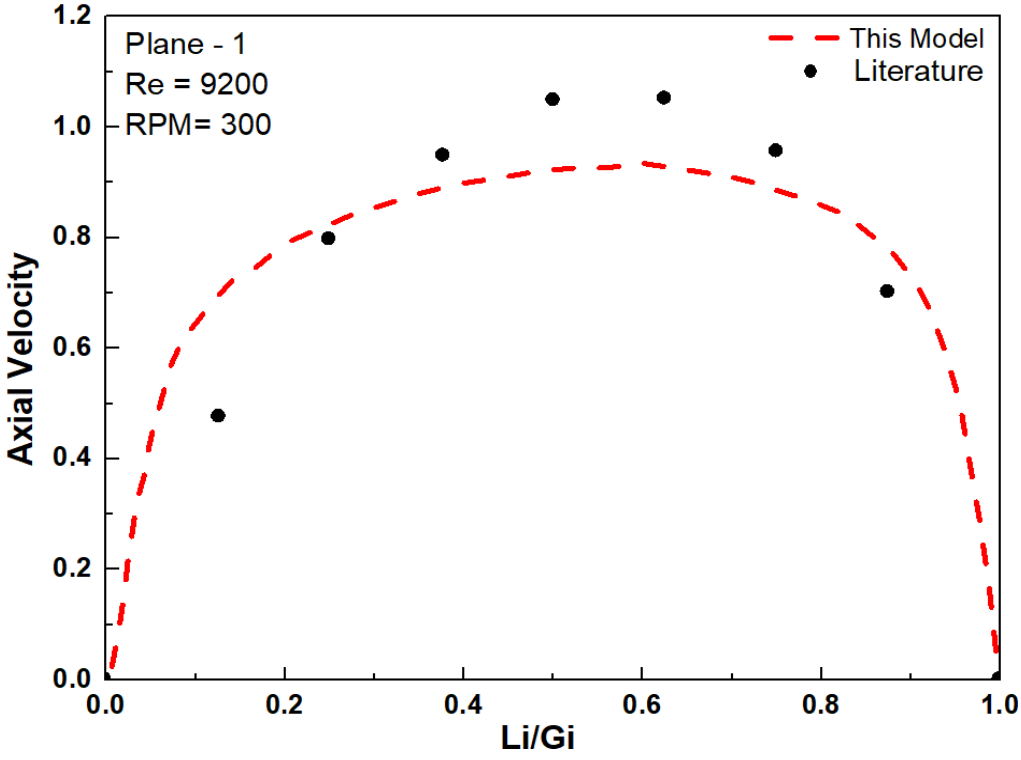


Figure 16 Axial mean velocities at plane-1; Re9300; RPM: 300

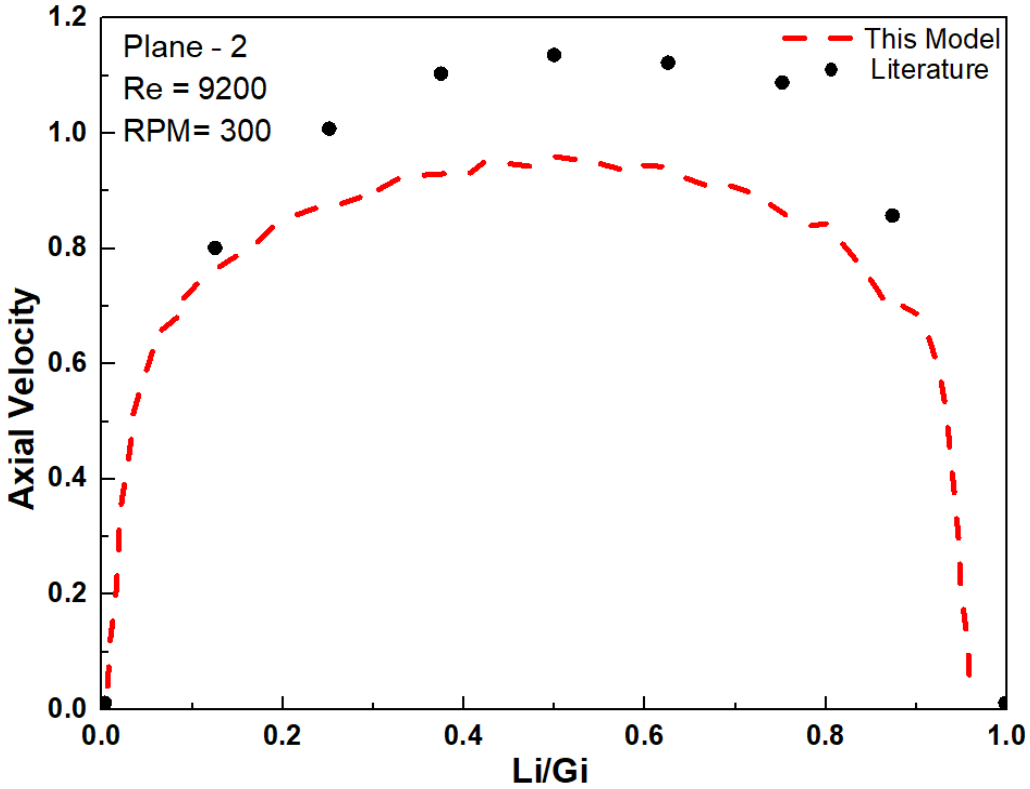

Figure 17 Axial mean velocities at plane-2; Re9200; RPM: 300

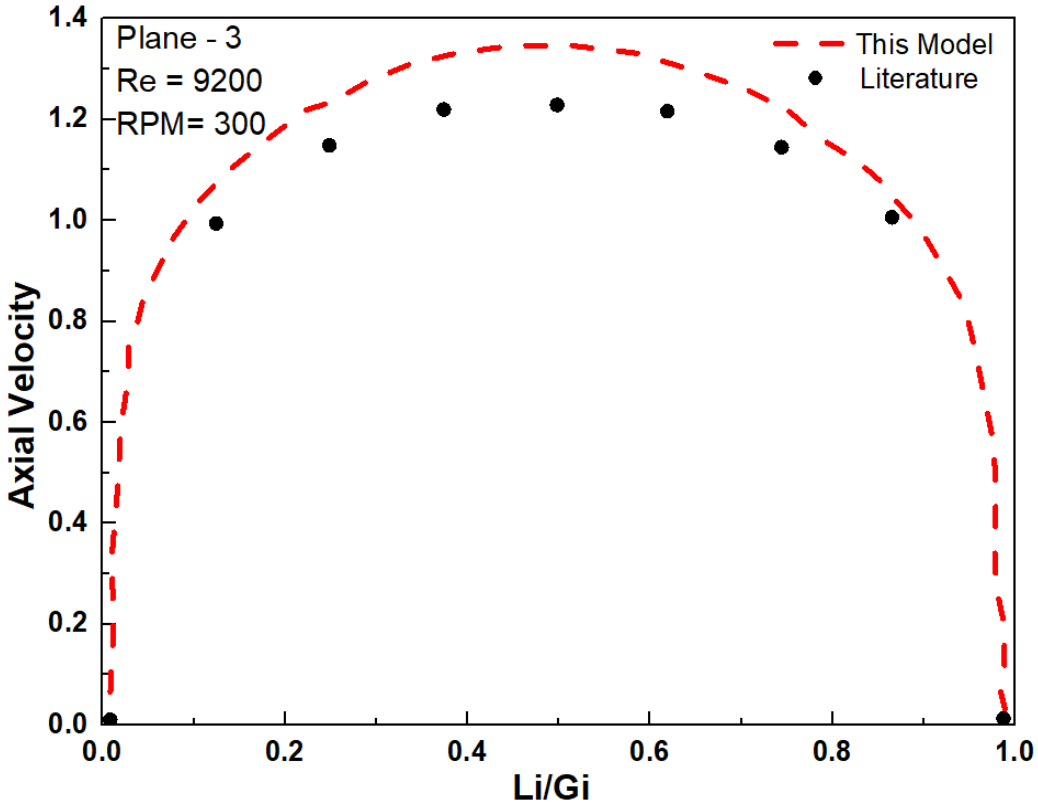

Figure 18 Axial mean velocities at plane-3; Re9200; RPM: 300

At the Rossby number 17.35 and Reynolds number of 9200 depicted by figures (16,17,18), which represents the axial mean velocities of all 03 planes for both 9300 and 9200 Reynolds number with 0 rpm and 300 rpm respectively. Minor differences have also been observed with and without rotation predominantly with lesser Rossby numbers, as the penetration was barred due to larger inertia of axial flow and swirl in the annulus's bulk region and hence rotational impact was limited. At lower Rossby number, no variation in the axial mean velocity profiles were manifested, near gap centers comprising of maximum velocities; rotating and non-rotating differences belonging to maximum velocities are higher at plane-1 and lower in plane-2 and plane-3. Also at lower Rossby numbers, radial velocities were found to be partial as in the latter case. A rapid decay near the inner wall and the larger values in the narrowest gap yielding slower decay in core region with the tangential velocity profiles shown in figures (19,20,21) & figures (22,23,24) representing the tangential mean velocities of all 03 planes for both 1150 and 9200 respectfully at Reynolds number at 300 rpm; and at such Rossby number, no counter- rotation was evidently perceived.

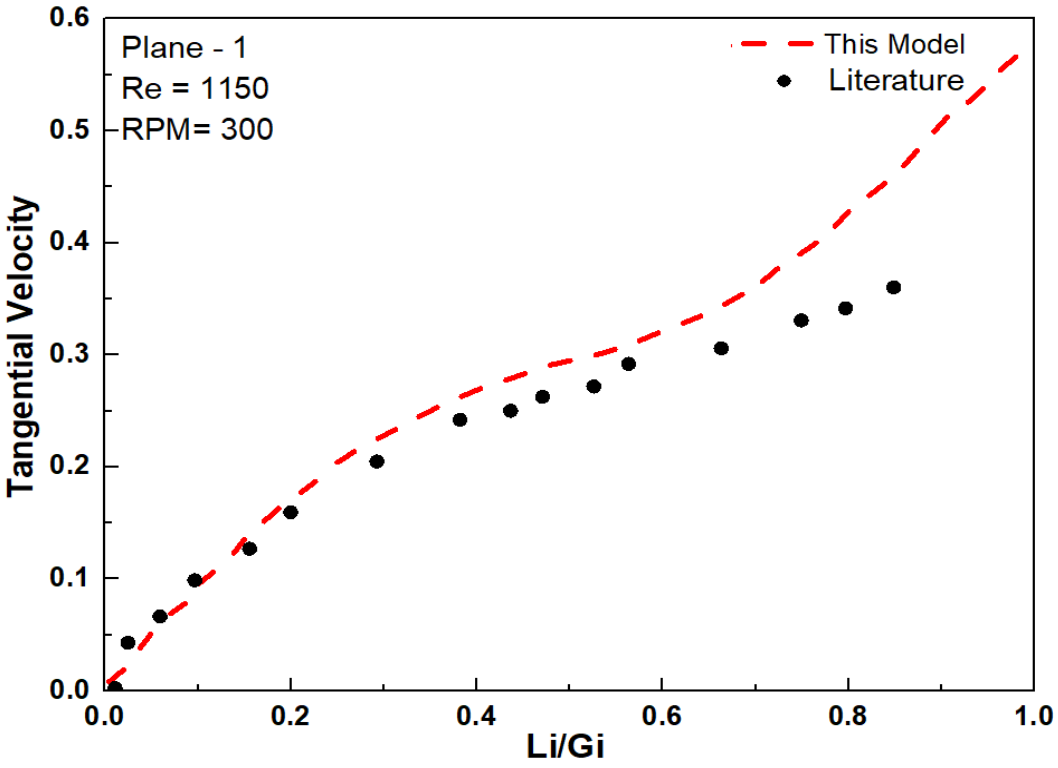


Figure 19 Tangential mean velocities at plane-1; Re:1150; RPM: 300

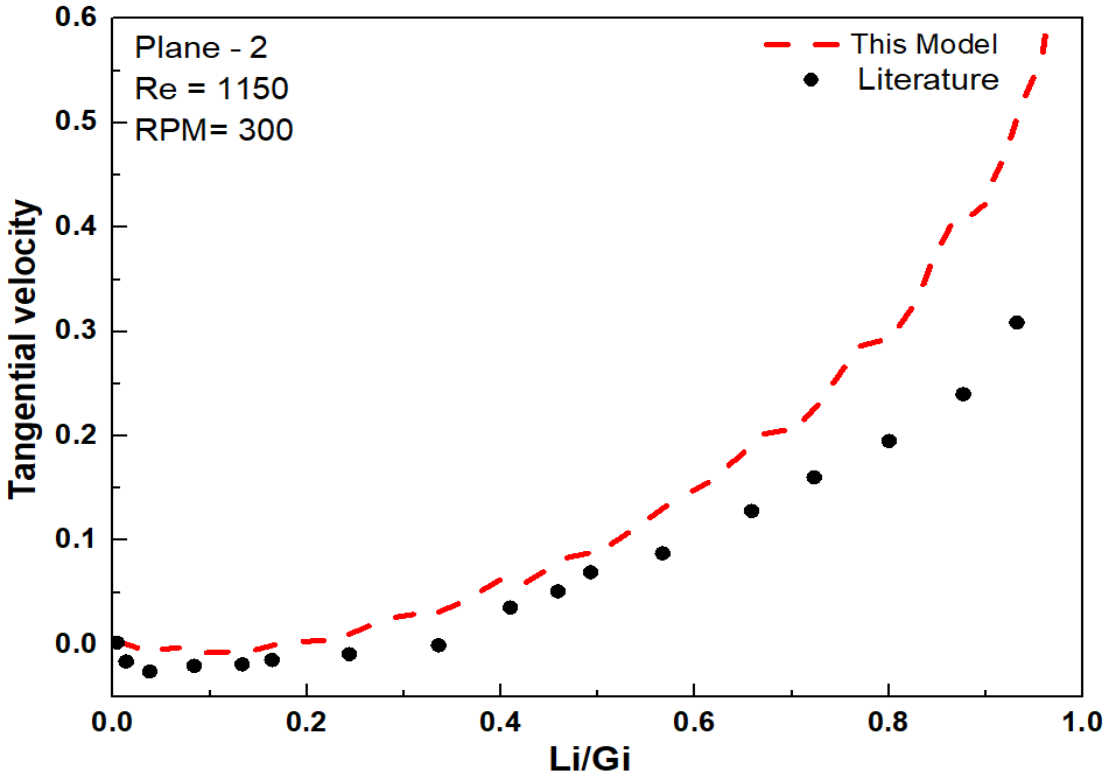


Figure 20 Tangential mean velocities at plane-2; Re:1150; RPM: 300

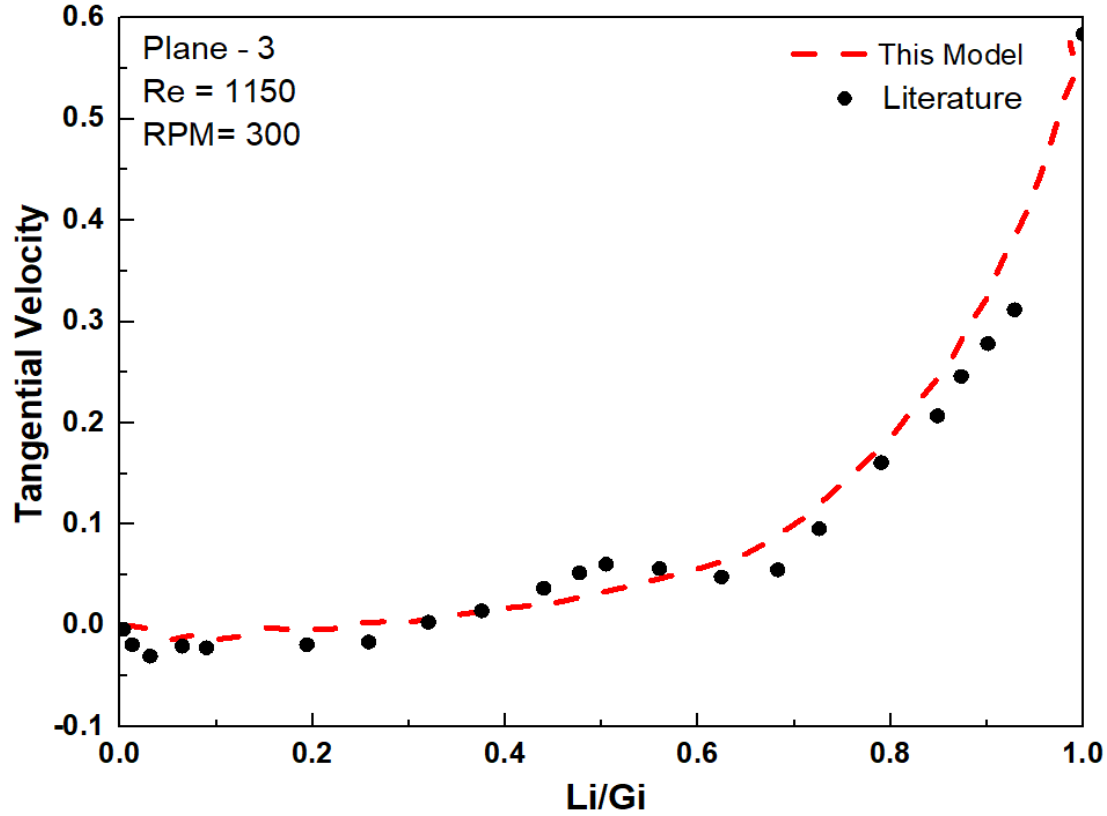


Figure 21 Tangential mean velocities at plane-3; Re:1150; RPM: 300

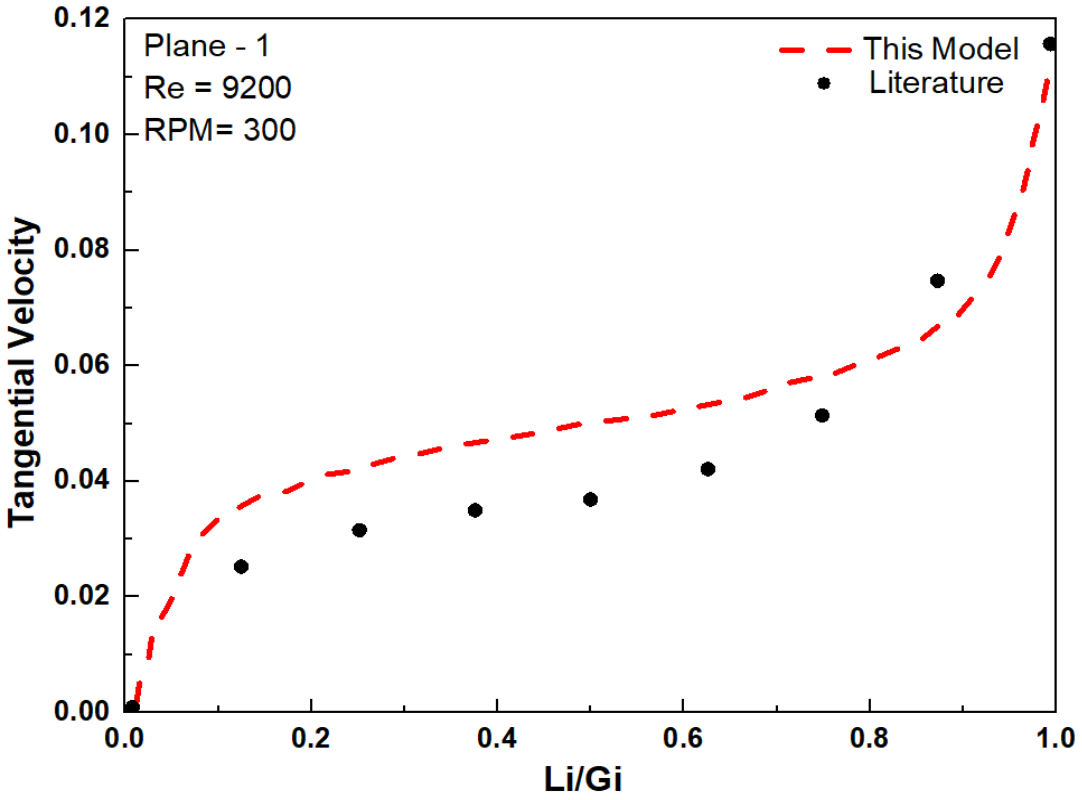


Figure 22 Tangential mean velocities at plane-1; Re:9200; RPM: 300

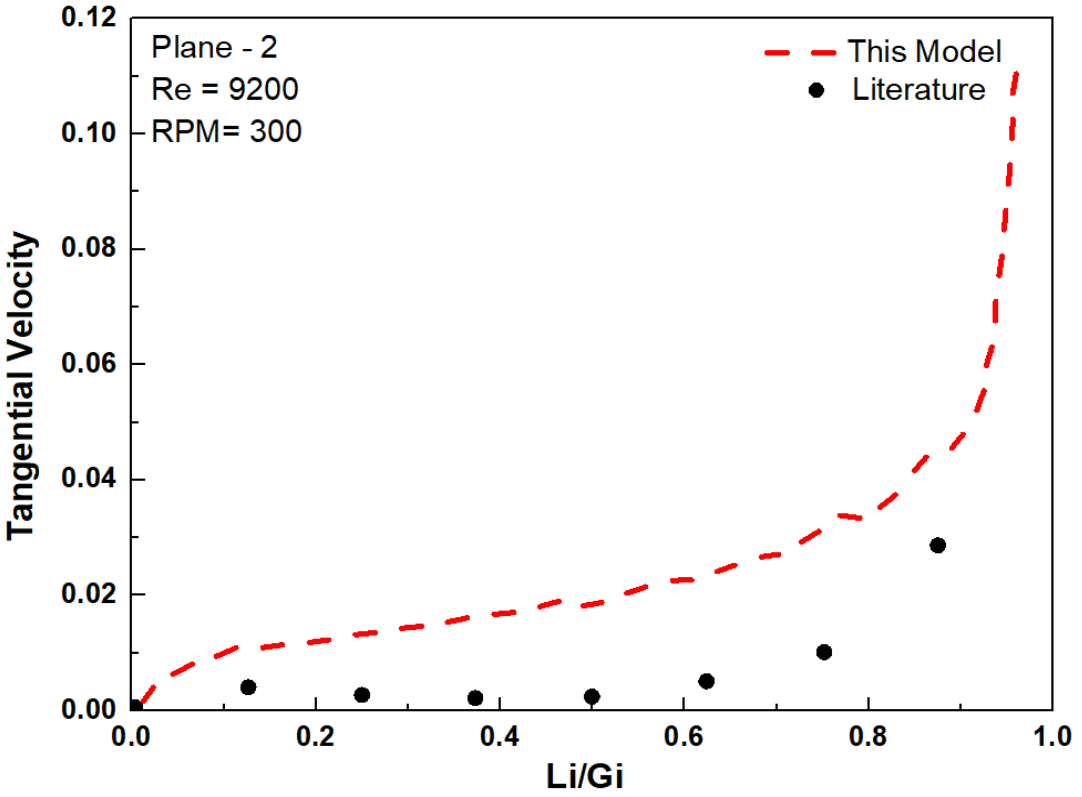


Figure 23 Tangential mean velocities at plane-2; Re:9200; RPM: 300

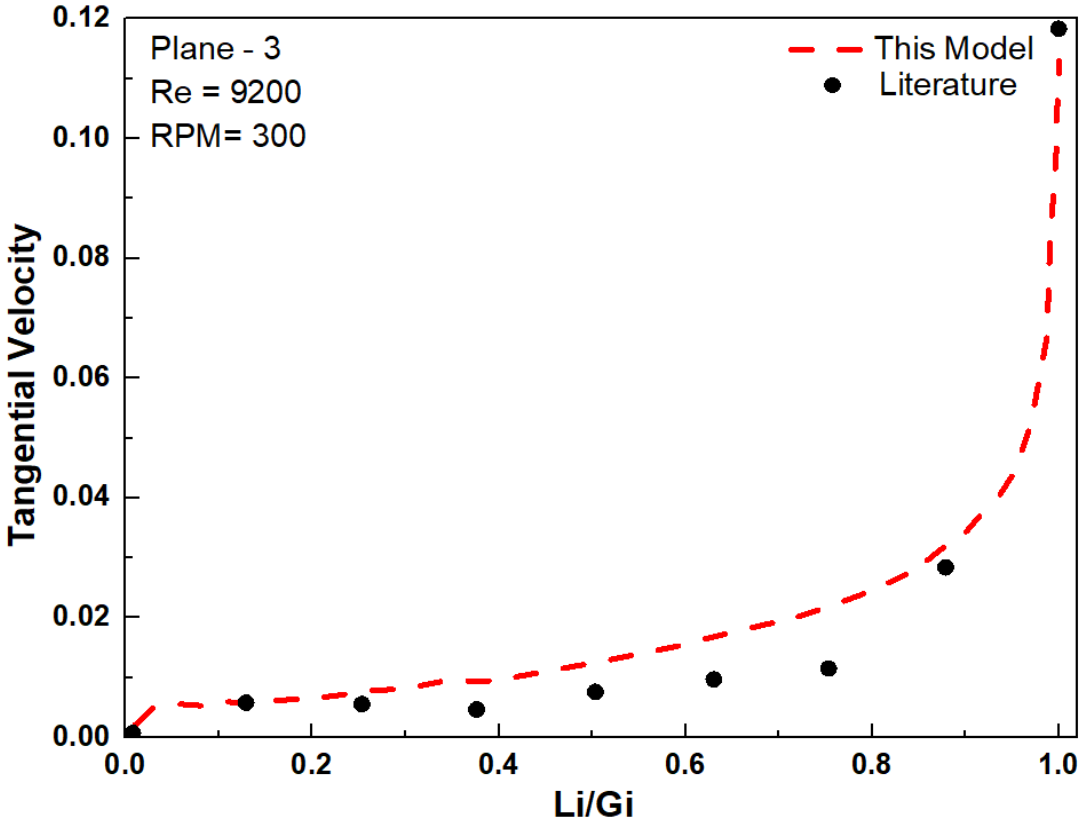


Figure 24 Tangential mean velocities at plane-3; Re:9200; RPM: 300

The comparison of mean tangential velocities can be revealed in figures (19-24) with the outer wall narrow or wide gap with rotational and non-rotational pipe having non-Newtonian fluid with the literature. As the Reynold or Rossby number was reduced, the tangential velocities were increased showing the inverse relation due to less impact of inertia. By decreasing the gap, the penetration of tangential velocities increased and hence those were primarily accumulated in the narrow gap and the Rossby number was increased simultaneously, and when the Rossby number was analogous for both rotational speeds, the tangential velocities also exhibited parallel trend.

Because of CMC solution elongation, the compression of turbulence intensities was occurred, which shows constant results in preceding experimental duct flow researches. By reduced Rossby number, the smaller variances for concentrations of turbulence having fluids of non-Newtonian behavior, with rotation makes the diffusion on tangential velocity through the bulk flow more convenient & operative, henceforth with the non-Newtonian fluid, turbulence intensities with overall increased cross-flow was prompted.

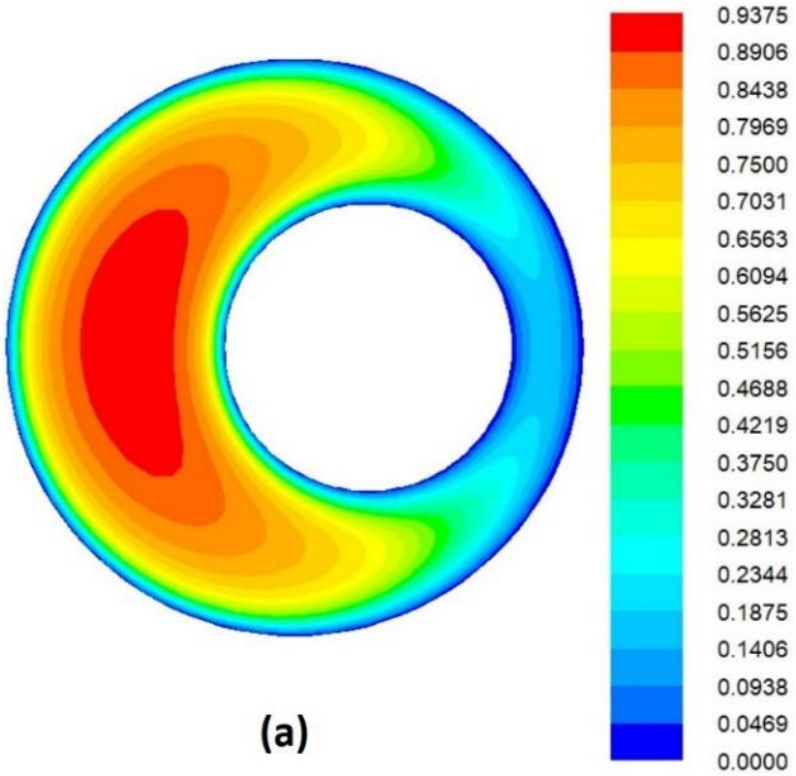


Figure 25 Velocity Magnitude contours at Re:1140;0rpm

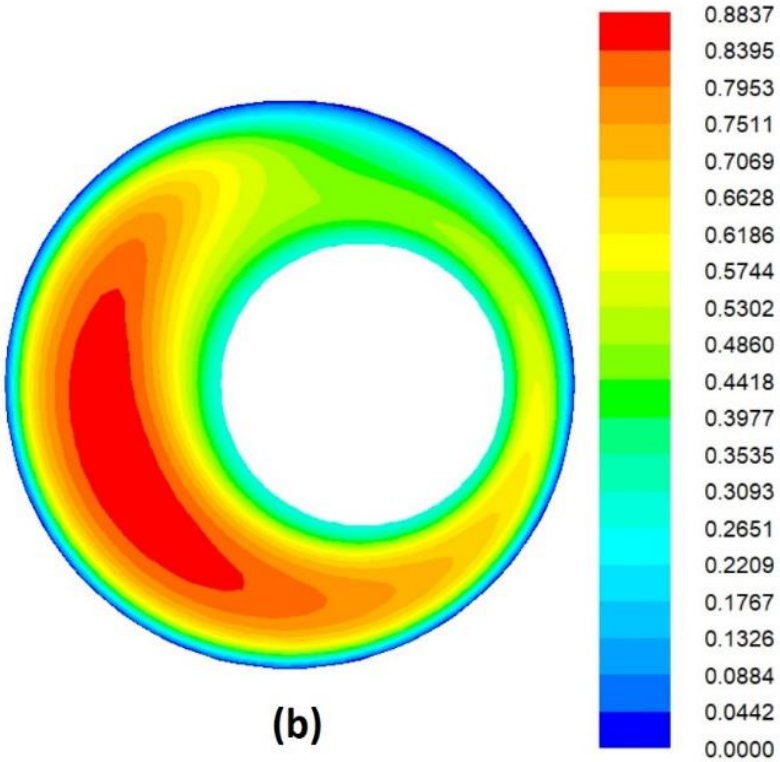


Figure 26 Velocity Magnitude contours at Re:1150;300rpm

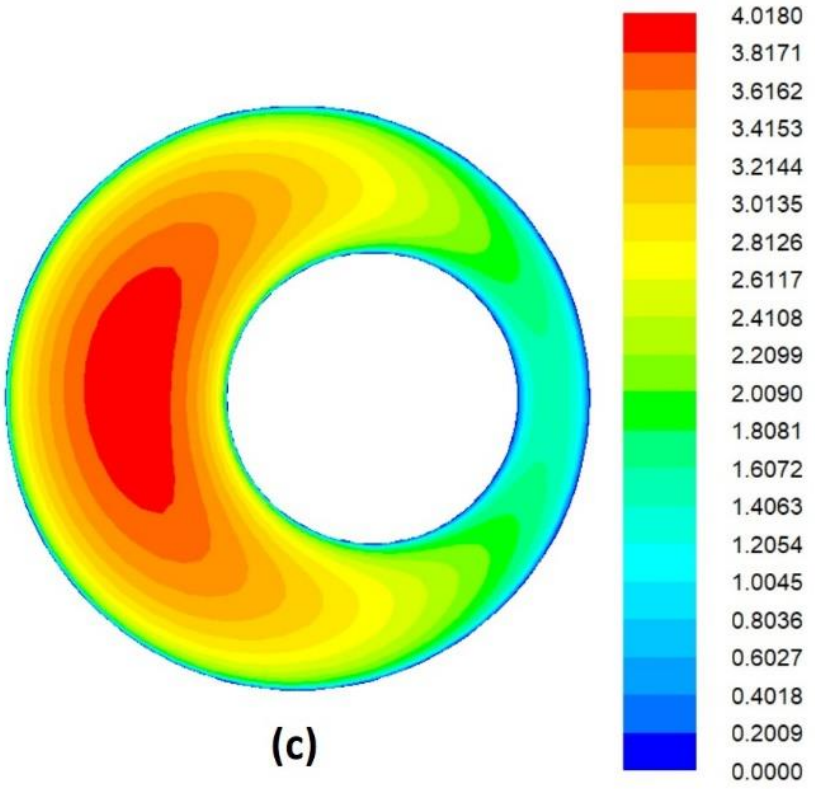


Figure 27 Velocity Magnitude contours at Re:9300;0rpm

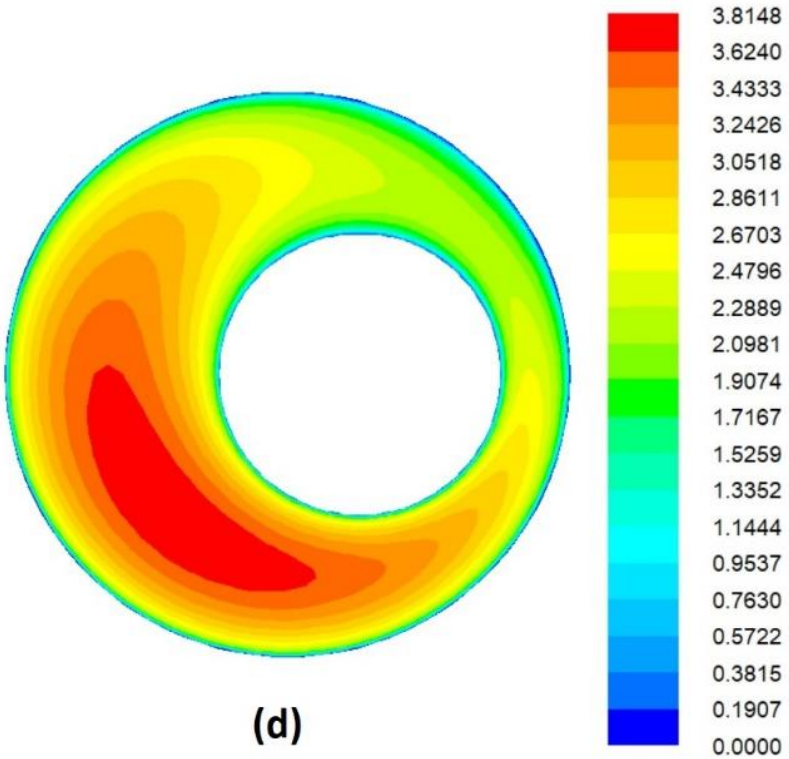


Figure 28 Velocity Magnitude contours at Re:9200;300rpm

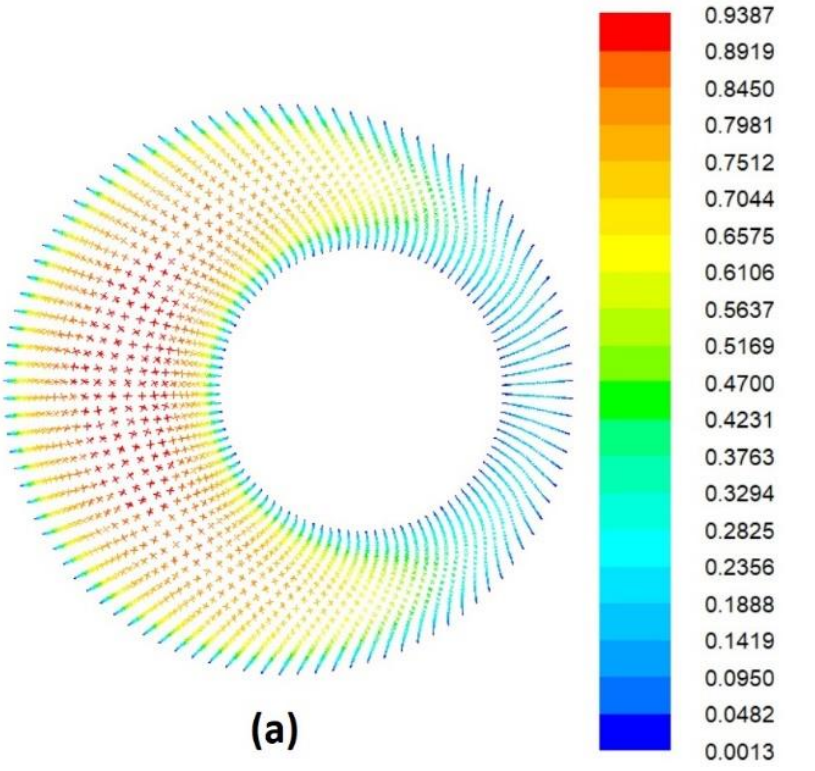


Figure 29 velocity vectors at Re:1140;0rpm

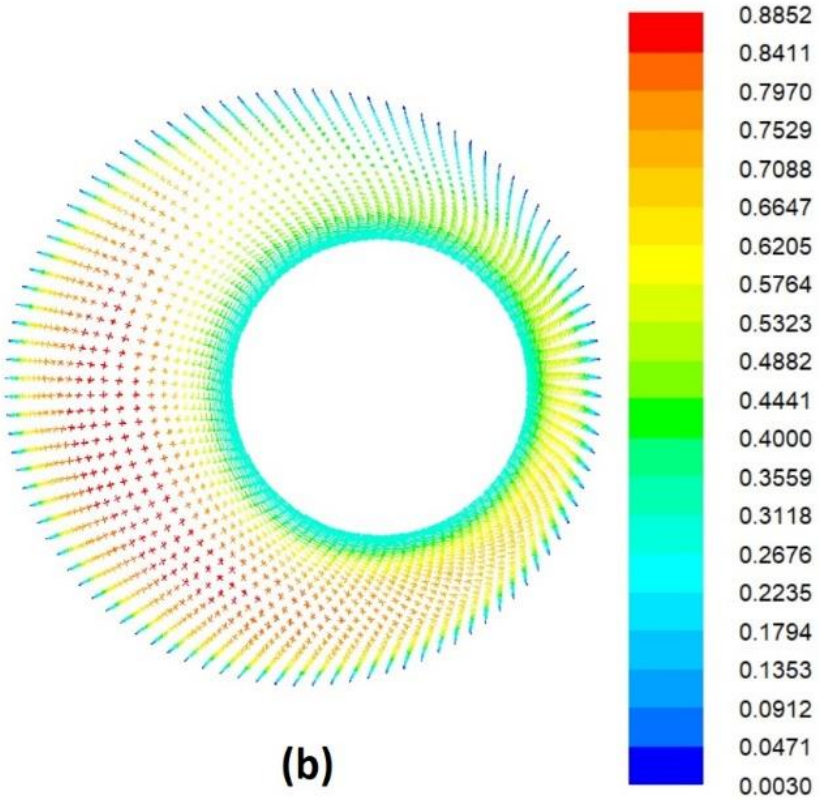


Figure 30 velocity vectors at Re:1150;300rpm

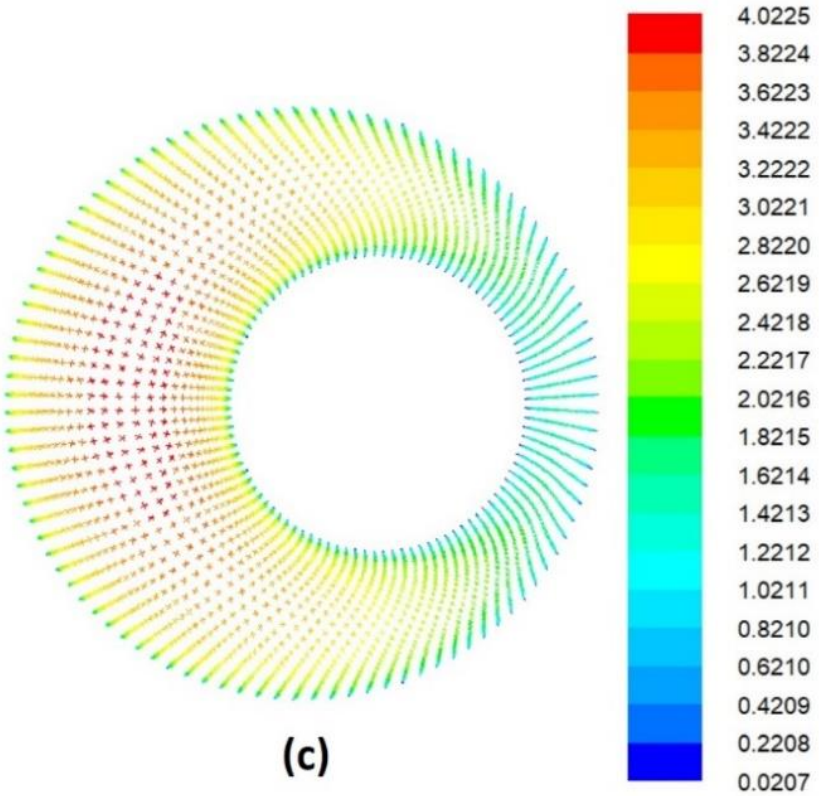


Figure 31 velocity vectors at Re:9300;0rpm

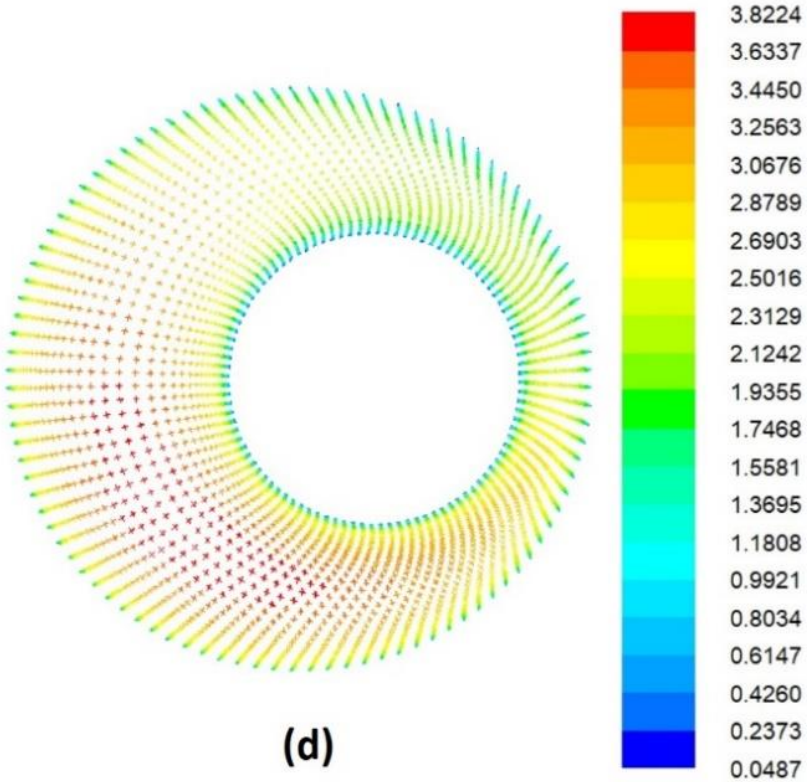


Figure 32 velocity vectors at Re:9200;300rpm

## 4.3 Fluid velocity effect on the flow in the drilling well:

The most important factor in the cutting transport process, annular velocity of drilling fluid plays an important role. The distribution of velocity in the drilling well were simulated for analyzing the effect of the inlet velocity. The fluid velocity vectors are illustrated in figures (29-32). The figure (30,32) shows the impact of velocity in the annulus having the constant drilling speed of 300 rpm, where non- rotational inner cylinder at 1140 Reynolds number, velocity vectors are shown in figure (29,31). Drill pipe rotation is perceptibly associated with the location of velocity magnitude core. Greater gap of annulus comprises of the maximum velocity and is transferred to the corner from that greater gap intermediate in counter clockwise direction. The spiral flow of drilling fluid by the annulus is obtained through the rotation of the drilling pipe, despite of the fact, by increasing the fluid velocity, the aforesaid effect reduces. Different patterns of the fluid velocities have been shown in the simulated results. The velocity magnitude contours are demonstrated in figures (25-28) through the drill pipe annulus. Larger gap of the annulus contains velocity core zone hence the effect of cutting accumulation on fluid velocity pattern can be assessed. Due to the accumulation of cuttings, low flow close to the lower side of the narrow gap is attained due to the accumulating confrontations. Velocity vectors shown in figures (29-32) depict further flow distributions. Additionally, due to such accumulations, the transformation of velocity core zone laterally deteriorates the path of drilling pipe rotation, therefore by increasing the fluid velocity the cutting accumulation declines. The particle concentration is lower as compared with the higher velocity of fluid. Due to higher inlet velocity the differences among the narrow and the wide gap increases through the annulus and subsequently the lodging time, in the narrowest gap become larger because of the massive cuttings transportation. The drag force exhibited on the cuttings is also increased by raising the fluid velocity, consequently additional cuttings passes through the fixed bed annuli.

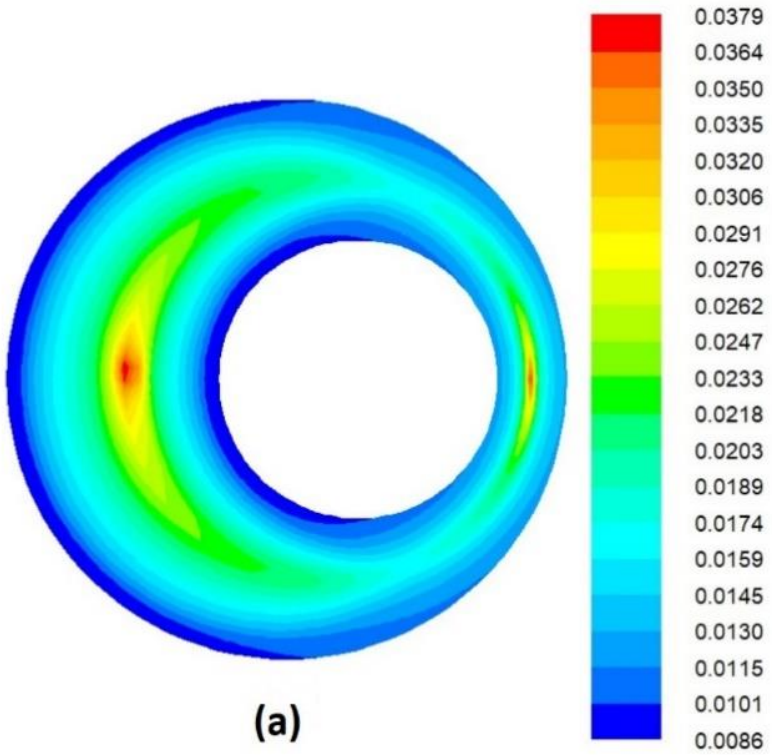


Figure 33 Molecular viscosity contours at Re:1140;0rpm

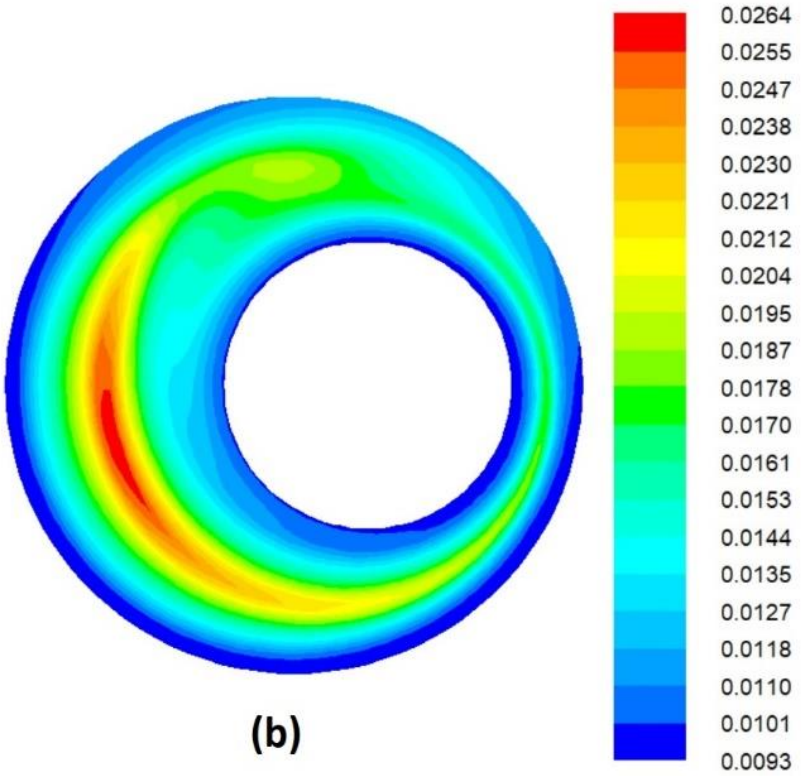


Figure 34 Molecular viscosity contours at Re:1150;300rpm

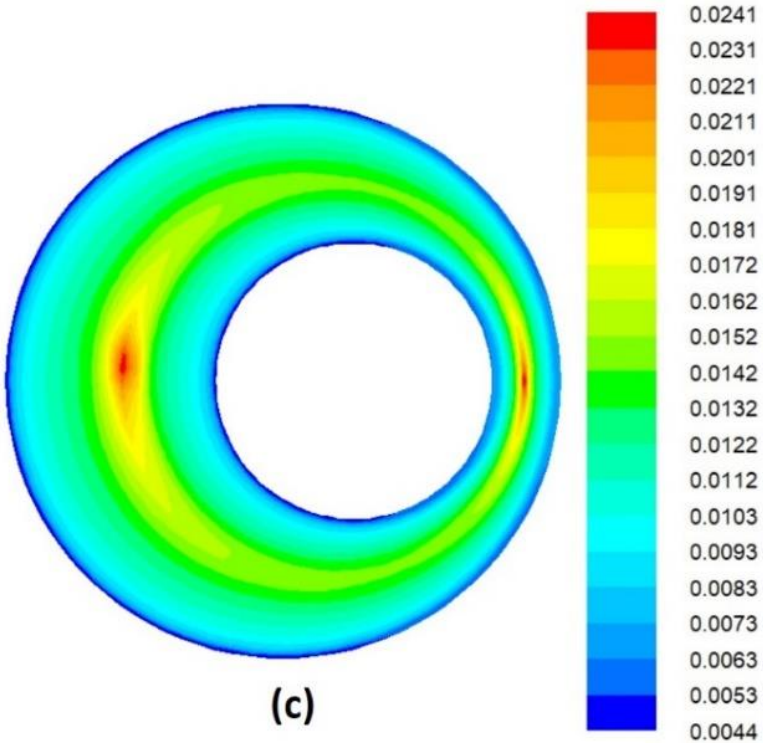


Figure 35 Molecular viscosity contours at Re:9300;0rpm

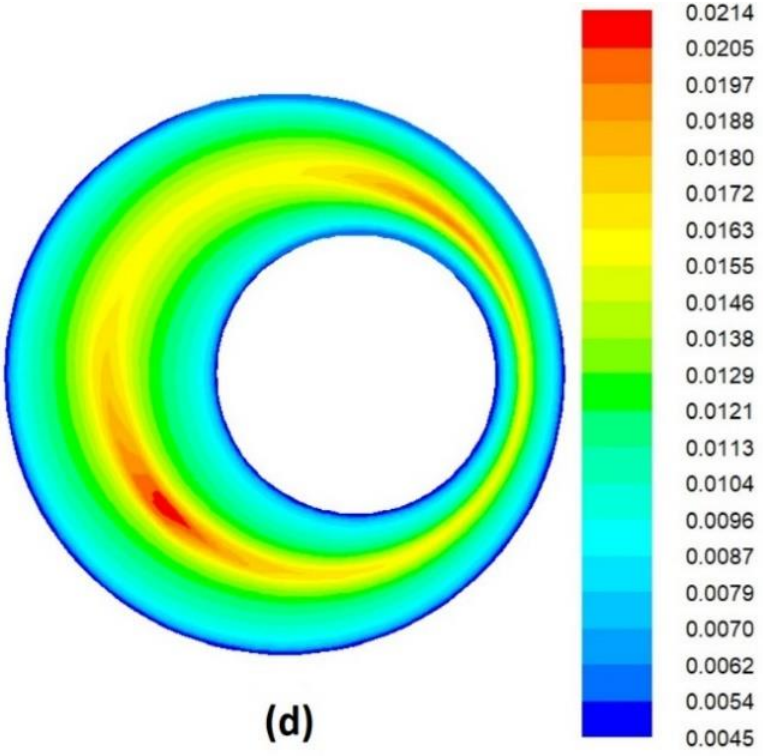


Figure 36 Molecular viscosity contours at Re:9200;300rpm

## 4.4 Impact of rotational speed on drilling fluid rheological properties

The shear thinning behavior of the fluid has also been perceived. The viscosity is high in the central part which is said to be low shear region and eventually less along the walls which are high shear regions.

Figures (33-36) represents the Molecular viscosity contours. The shear thinning behavior of the fluid can be observed from the contours. The viscosity is smaller near the walls (high shear regions) and it is greater in the central part (low shear regions of the annulus).

Typically, non- Newtonian comportment is reveled from the drilling fluids, such that shear rate and shear stress is non-linearly associated. The simulated rheological model signifies the impact associated to the turbulence of the drilling fluid. To define the rheology to drill fluid, Bukley-Hershel, Power-law, and Bingham-plastic. Shear rates of the drilling fluids related to wellbore annulus, are effectively defined by the power-law [22]. Higher granular temperature along the drilling pipe wall is observed through the simulations which is demonstration of the fact that energy transfer is occurred between the cuttings and the rotational drill pipe. Due to high shear rate along the drill pipe, cuttings collisional interface is amplified [14]. Feebler variations of cutting have been observed as the length of the drilling pipe wall is enhanced due to low shear rates, consequently granular temperature is decreased. The likelihood of cuttings collision in the upper side of the annuli is lower owing to cuttings low volumetric fractions, resulting in granular temperature at lower range [33]. Cuttings high volumetric fractioned fixed bed is formed at the bottom of the wall casing. Current simulations are based on the experimental verdicts. Moreover, drag force affected on the cuttings is predominantly affected by the rheological properties of the drill-fluid. It can be noted from equation 17 that cuttings high drag force can be occasioned through high seeming viscosity. Therefore, higher seeming viscosity drill fluid scrubs the annuli bottom from cuttings and vice versa with the lower seeming viscosity situations.

## 4.5 Newtonian fluid rotational flow

Results related to axial average velocities with counter-clockwise rotation, a bulk Reynolds number and Rossby number of 9000 & 4.6 are depicted in figures (38-41).

The axial average velocities of the Newtonian fluid with rotation at planes 2 and 3 are smaller as compare to the plane-1 as depicted in figures (38-41). The variations in the highest velocities of rotational & irrotational flows decreases in quadrants 1 to 3 and then increases in quadrant 4. Whereas in irrotational flows, maximum velocities amongst the openings (narrow & wide), is larger when compared with a difference with rotation at planes 1 and 3. The non-uniform change in plane 2 can be seen significant in velocity profile of rotational flow and the maximum velocities are not achieved in the location close to inner & outer walls of the gap centers, respectively. At planes 2 and 3, the axial mean velocities of the Newtonian fluid are smaller with rotation as compare to those of the stationary flow. While the axial mean velocities are higher between planes-1. The axial mean velocities with and without rotation become identical between plane-1.

At planes 1 and 3, the radial mean velocities of the rotating flows are about two percent of the bulk velocity with negative values near the center of the outer pipe. The radial mean velocities near the inner wall for the rotating flows increase to twelve percent of the bulk velocity in plane 2 which is due to the transfer of the max. axial velocity in the plane. While at side of inner rotating wall, tangential velocity effect on the bulk flow is minimized with an increased gap b/w the cylinders. It has been seen from figures (43-44), that strong tangential exists in the narrow gap with the increase in values of radial mean velocities to 30% and 15% of bulk velocities close to the inner and outer walls, respectively. This variation of tangential velocity decreases with gap width in contrast with the axial mean velocity which is due to the variation in the local Rossby number and the lowest value of Rossby number is in the narrowest space of annuli. The velocity magnitude contours are demonstrated in figures (37 & 38) through the drill pipe annulus, belongs represents velocity magnitude at 9000 Reynolds number with non-rotated & rotated flow at 300 RPM respectively. Larger gap of the annulus contains velocity core zone hence the effect of cutting accumulation on fluid velocity pattern can be assessed For the Newtonian fluid glycerin was taken as Newtonian fluid at the atmospheric conditions.

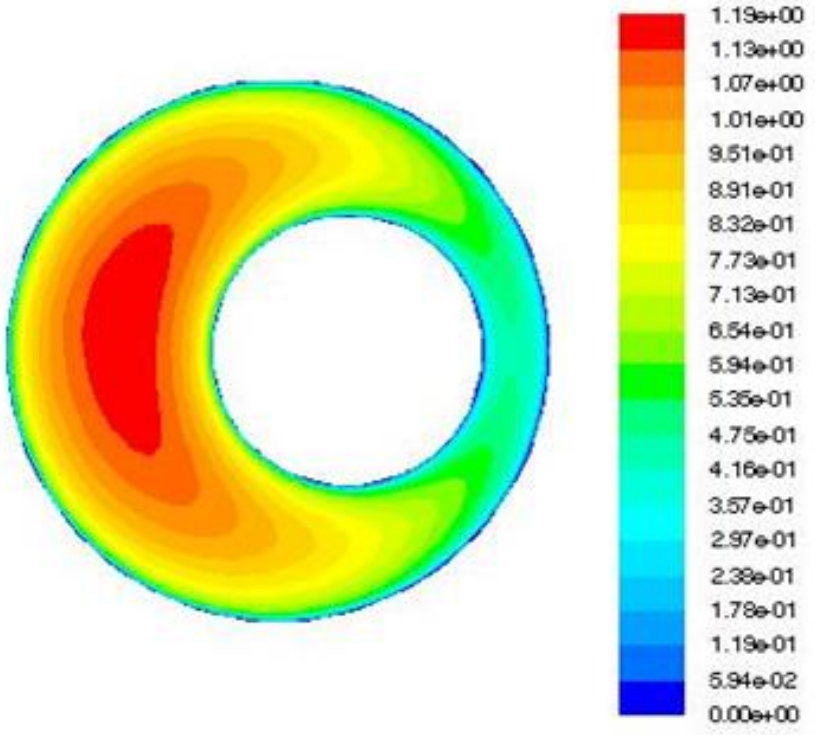


Figure 37 Velocity Magnitude contours at Re:9000; 0rpm

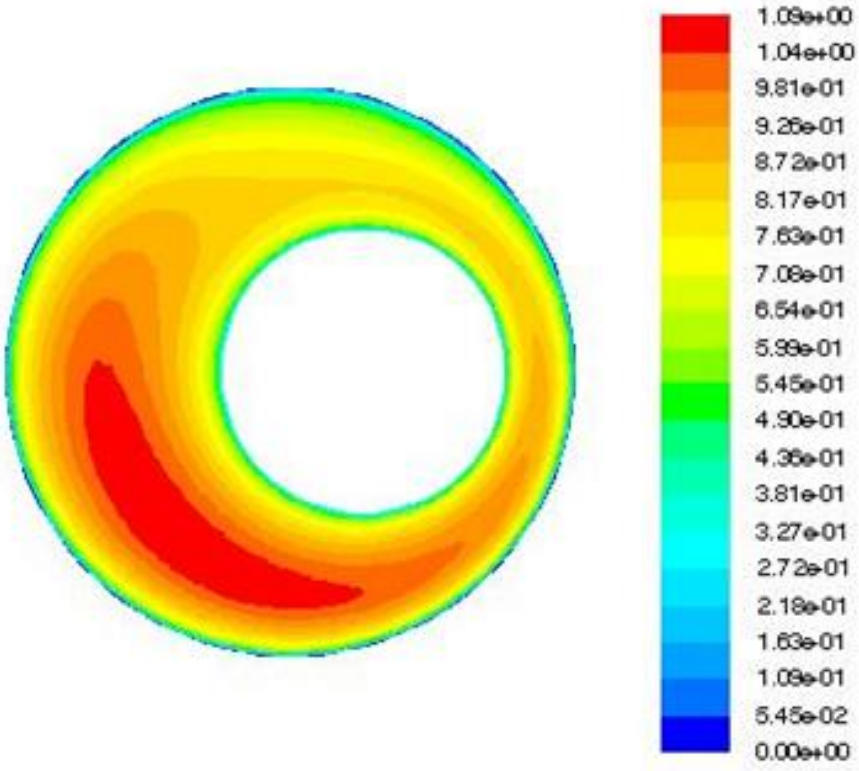


Figure 38 Velocity Magnitude contours at Re:9000;300rpm

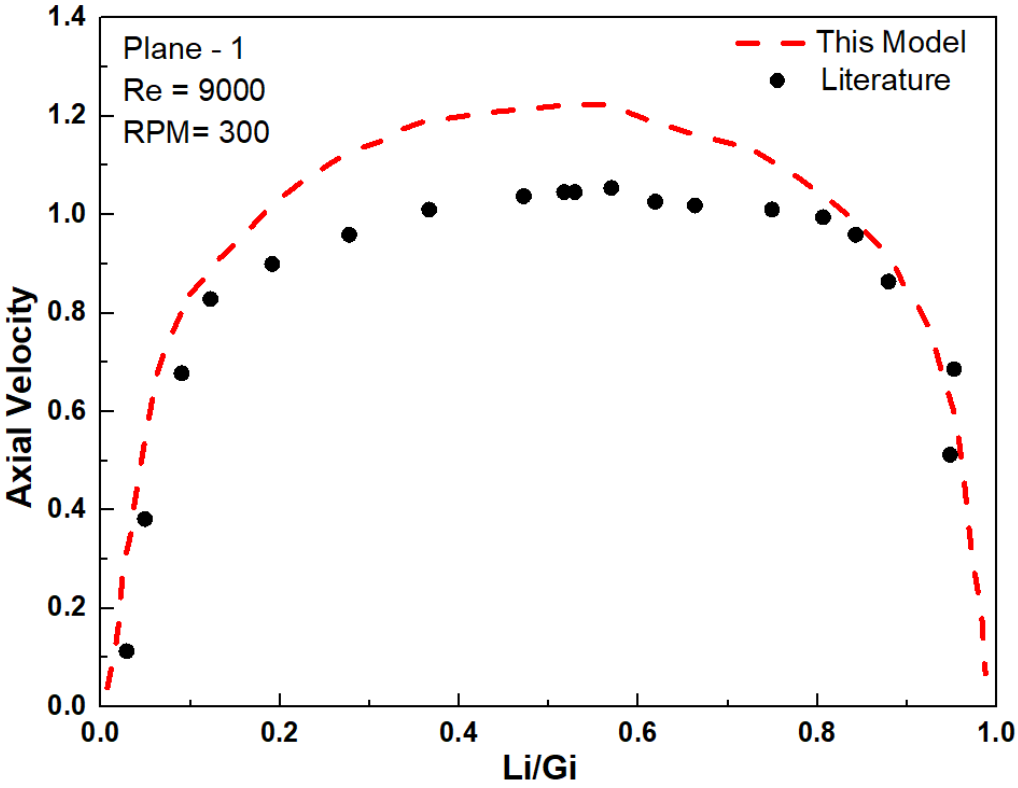


Figure 39 Axial Mean velocities at Plane-1; Re: 9000; RPM:300

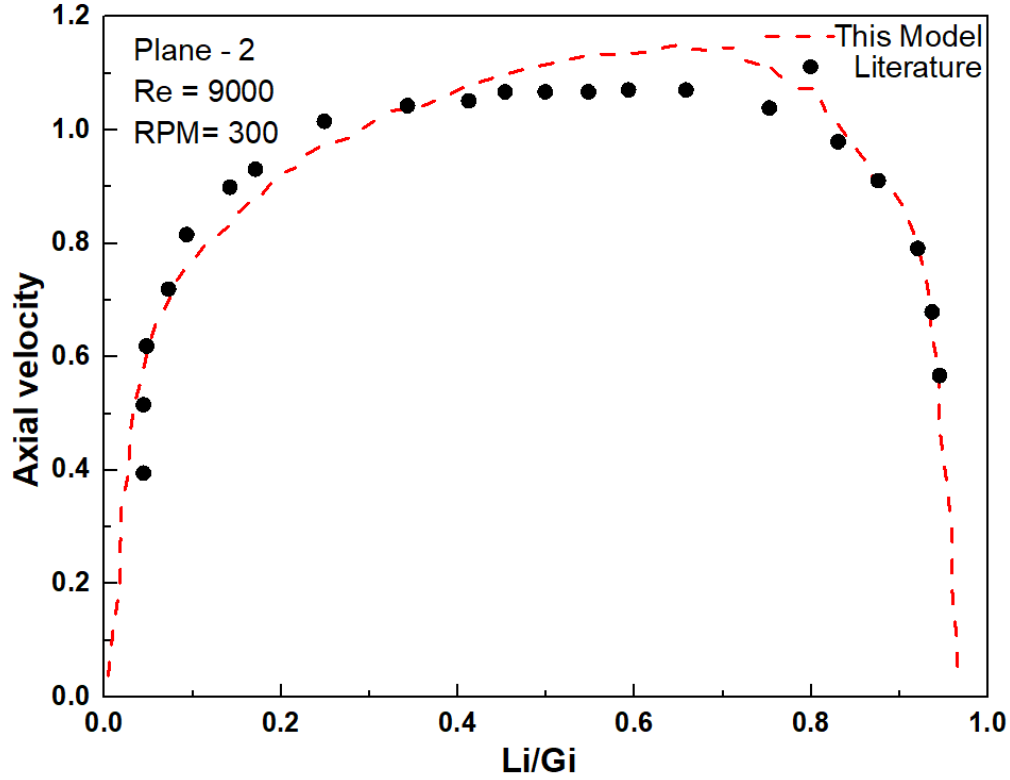


Figure 40  Axial Mean velocities at Plane-2; Re: 9000; RPM:300

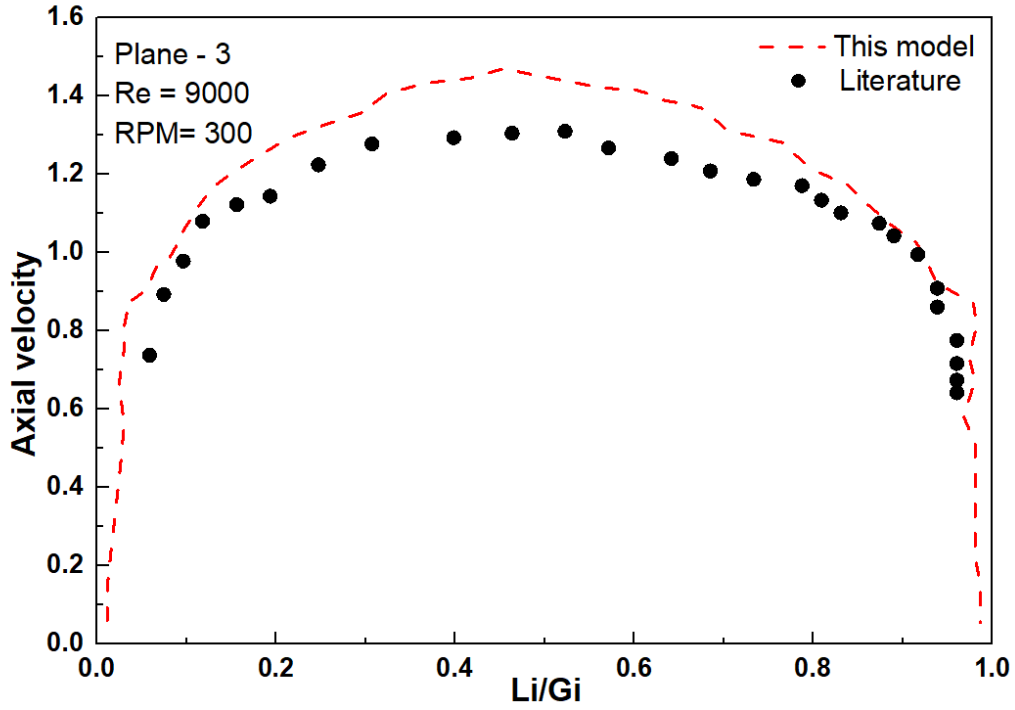


Figure 41 Axial Mean velocities at Plane-3; Re: 9000; RPM:300

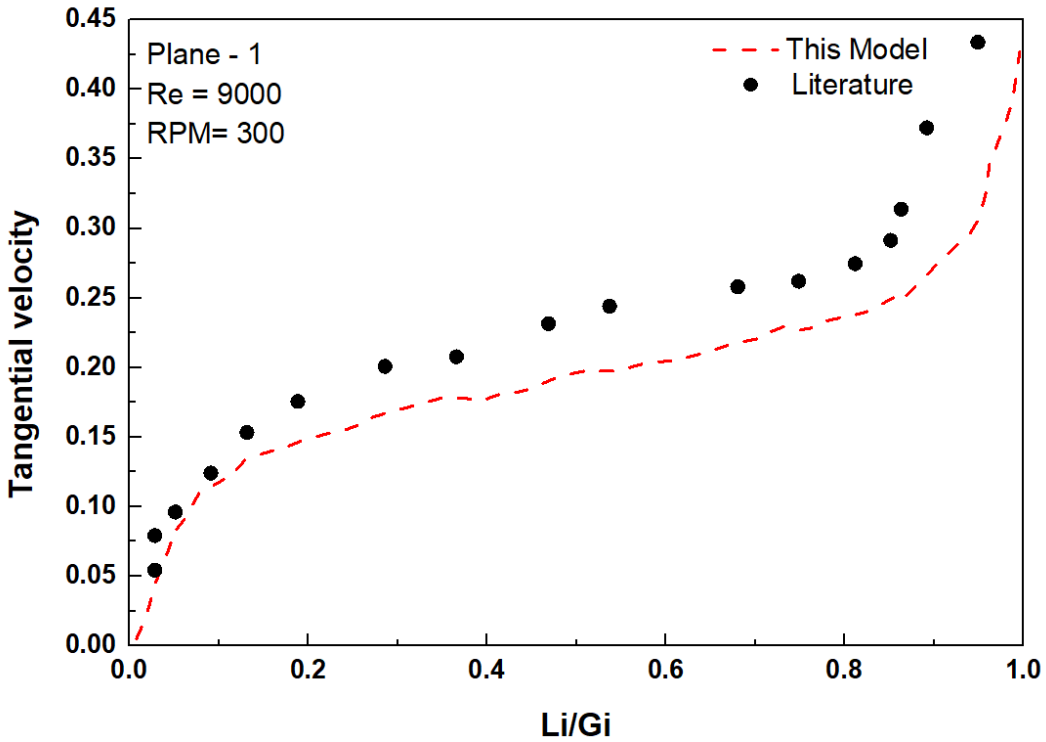


Figure 42 Tangential Mean velocities at Plane-1; Re: 9000; RPM:300

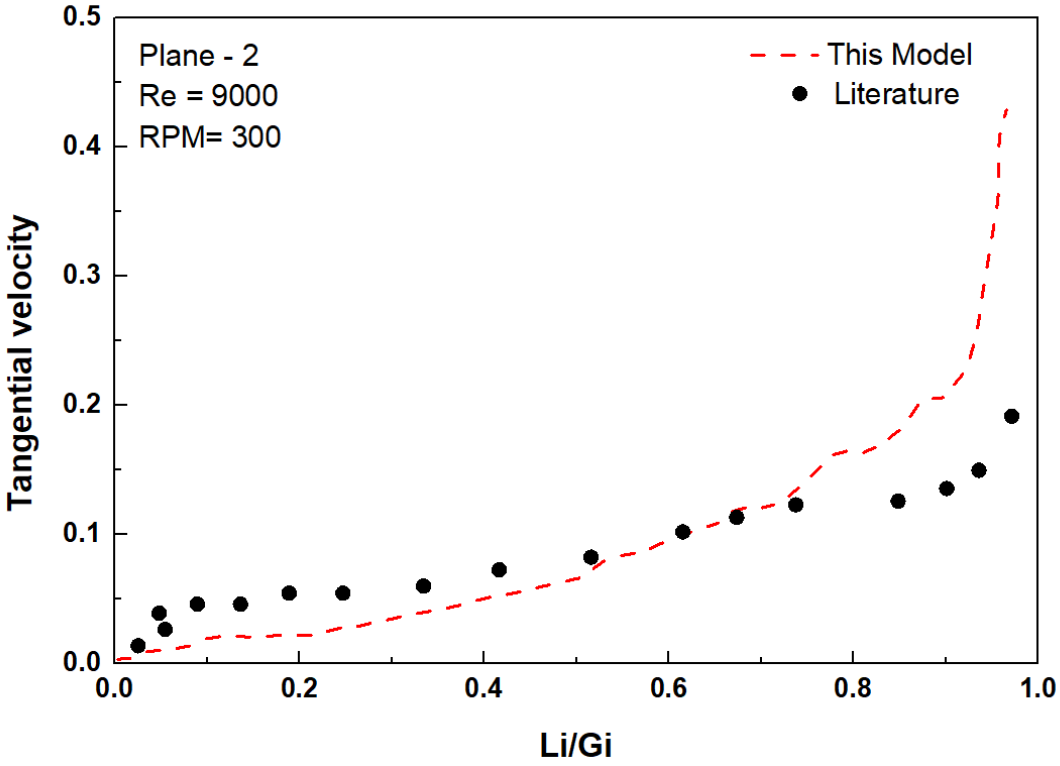


Figure 43Tangential Mean velocities at Plane-2; Re: 9000; RPM:300

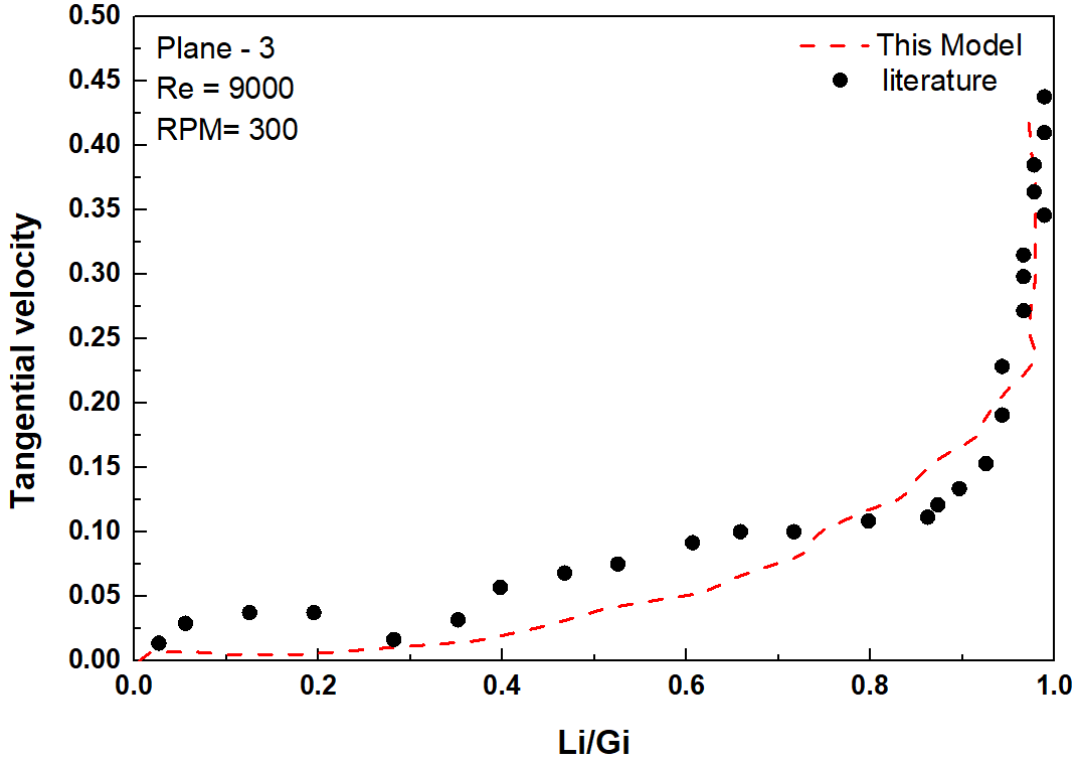


Figure 44 Tangential Mean velocities at Plane-3; Re: 9000; RPM:300

# Chapter 5

# Conclusions and Future Recommendations

## 5.1 Conclusion

For the simulations of cuttings and non-Newtonian fluids in an annulus are grounded on the kinetic theory for the granular flow, which is subjected for the CFD model. Simulations of the non-Newtonian fluid having single phase are valid with the experimental work originated in the literature.

The impacts of the velocity of annuli, drill pipe rotation and characteristics of drill fluid rheology have been investigated. Cuttings transport is upgraded through the rotation of the drilling pipe. The circulations of the mean axial velocity with large fluctuations in cross flow mean velocity, become more uniform along the wall of the annulus and eventually abridged by raising the Robby number or bulk velocity of the fluid. Near the inner wall of the annulus, the radial circulation declined swiftly by reducing the Rossby number, resulting in even profile for the tangential mean velocity. Maximum values were perceived in the narrowest gap for the angular circulations. At the least Reynolds number, the resistance to flow of fluid was raised, while at high Reynolds number it was unaffected. It was noticed that, at about 9200 Reynolds number, the drag reduction for the CMC solution with the leeway of nonturbulent flow has been reported and at large turbulences, steady results were observed. Rotation with the CMC, triggered a counter rotating tangential flow near outer wall pipe with increased Reynolds number at about 9200, such counter rotating flow was lost.

## 5.2 Future Recommendations

The results attained in this work is consisted of basic conditions such as system is free from the pores or any cracks in borehole over whole length of the pipe simulated, inner pipe dimeter, atmospheric pressure and temperature. Additional research will be emphasized on the facts of the tool joint structures, leakage or passing of fluids from the borehole into the open hole segment of ground during conveyance of cuttings to the surface.

# References

[1] Geothermie Zentrum Bochum. Geothermal Energy, in, 2014.

[2] R.A. Tersa, Improvements of cuttings transport models through physical experiments and numerical investigations of solid-liquid transport, Papierflieger Verlag GmbH, 2016.

[3] E.B. Nelson, Well cementing, Newnes, 1990.

[4] C. Sauer, Mud displacement during cementing state of the art, Journal of Petroleum Technology, 39 (1987) 1,091-091,101.

[5] S. Pelipenko, Displacement flow of non-newtonian fluids in an eccentric annulus, in, University of British Columbia, 2002.

[6] K.C. Wilson, G.R. Addie, A. Sellgren, R. Clift, Slurry transport using centrifugal pumps, Springer Science & Business Media, 2006.

[7] C.T. Crowe, Multiphase flow handbook, CRC press, 2005.

[8] B. Swanson, J. Heritage, D. Lawson, Wellbore Fluids Model Provides Basis for Drilling Optimization, in: SPE Annual Technical Conference and Exhibition, Society of Petroleum Engineers, 1991.

[9] M. Allouche, I. Frigaard, G. Sona, Static wall layers in the displacement of two visco-plastic fluids in a plane channel, Journal of Fluid Mechanics, 424 (2000) 243-277.

[10] N.A. Barton, G.L. Archer, D.A. Seymour, Computational fluid dynamics improves liner cementing operation, in: International Journal of Rock Mechanics and Mining Sciences and Geomechanics Abstracts, 1995, pp. 165A.

[11] R. Clark, K. Bickham, A mechanistic model for cuttings transport, in: SPE Annual Technical Conference and Exhibition, Society of Petroleum Engineers, 1994.

[12] S. Bittleston, J. Ferguson, I. Frigaard, Mud removal and cement placement during primary cementing of an oil well–Laminar non-Newtonian displacements in an eccentric annular Hele-Shaw cell, Journal of Engineering Mathematics, 43 (2002) 229-253.

[13] T. Yan, K. Wang, X. Sun, S. Luan, State-of-the-Art Hole-Cleaning Techniques in Complex Structure Wells, Recent Patents on Engineering, 8 (2014) 50-57.

[14] B. Pang, S. Wang, Q. Wang, K. Yang, H. Lu, M. Hassan, X. Jiang, Numerical prediction of cuttings transport behavior in well drilling using kinetic theory of granular flow, Journal of Petroleum Science and Engineering, 161 (2018) 190-203.
[15] B. Pang, S. Wang, G. Liu, X. Jiang, H. Lu, Z. Li, Numerical prediction of flow behavior of cuttings carried by Herschel-Bulkley fluids in horizontal well using kinetic theory of granular flow, Powder Technology, 329 (2018) 386-398.
[16] D. Kumar, K. Ramesh, S. Chandok, Effectiveness of magnetic field on the flow of Jeffrey fluid in an annulus with rotating concentric cylinders, Journal of the Brazilian Society of Mechanical Sciences and Engineering, 40 (2018) 305.
[17] B.S. Yilbas, M. Yürüsoy, M. Pakdemirli, Entropy analysis for non-Newtonian fluid flow in annular pipe: constant viscosity case, Entropy, 6 (2004) 304-315.
[18] H. Teimouri, G.A. Sheikhzadeh, M. Afrand, M.M. Fakhari, Mixed convection in a rotating eccentric annulus containing nanofluid using bi-orthogonal grid types: a finite volume simulation, Journal of Molecular Liquids, 227 (2017) 114-126.
[19] M. Shirazi, A. Shateri, M. Bayareh, Numerical investigation of mixed convection heat transfer of a nanofluid in a circular enclosure with a rotating inner cylinder, Journal of Thermal Analysis and Calorimetry, (2018) 1-13.
[20] S. Akhshik, M. Behzad, M. Rajabi, CFD–DEM approach to investigate the effect of drill pipe rotation on cuttings transport behavior, Journal of Petroleum Science and Engineering, 127 (2015) 229-244.
[21] X. Sun, K. Wang, T. Yan, S. Shao, J. Jiao, Effect of drillpipe rotation on cuttings transport using computational fluid dynamics (CFD) in complex structure wells, Journal of Petroleum Exploration and Production Technology, 4 (2014) 255-261.
[22] S.-m. Han, N.-s. Woo, Y.-k. Hwang, Solid-liquid mixture flow through a slim hole annulus with rotating inner cylinder, Journal of mechanical science and technology, 23 (2009) 569-577.
[23] J. Nouri, J. Whitelaw, Flow of Newtonian and non-Newtonian fluids in an eccentric annulus with rotation of the inner cylinder, International Journal of Heat and Fluid Flow, 18 (1997) 236-246.
[24] O. Heydari, E. Sahraei, P. Skalle, Investigating the impact of drillpipe's rotation and eccentricity on cuttings transport phenomenon in various horizontal annuluses using computational fluid dynamics (CFD), Journal of Petroleum Science and Engineering, 156 (2017) 801-813.

[25] G. Liu, P. Wang, H. Lu, F. Yu, Y. Zhang, S. Wang, L. Sun, Numerical prediction of flow hydrodynamics of wet molecular sieve particles in a liquid-fluidized bed, Particuology, 25 (2016) 42-50.
[26] M. Hadžiabdić, K. Hanjalić, R. Mullyadzhanov, LES of turbulent flow in a concentric annulus with rotating outer wall, International Journal of Heat and Fluid Flow, 43 (2013) 74-84.
[27] A. Maleki, I. Frigaard, Primary cementing of oil and gas wells in turbulent and mixed regimes, Journal of Engineering Mathematics, 107 (2017) 201-230.
[28] A. Murata, K. Iwamoto, Heat and fluid flow in cylindrical and conical annular flow-passages with through flow and inner-wall rotation, International Journal of Heat and Fluid Flow, 32 (2011) 378-391.
[29] I. Bicalho, D. dos Santos, C. Ataíde, C. Duarte, Fluid-dynamic behavior of flow in partially obstructed concentric and eccentric annuli with orbital motion, Journal of Petroleum Science and Engineering, 137 (2016) 202-213.
[30] M. Ebrahimi, M. Crapper, J.Y. Ooi, Numerical and experimental study of horizontal pneumatic transportation of spherical and low-aspect-ratio cylindrical particles, Powder Technology, 293 (2016) 48-59.
[31] L. Sheng, Y. Tai, C. Kuo, S. Hsiau, A two-phase model for dry density-varying granular flows, Advanced Powder Technology, 24 (2013) 132-142.
[32] L. Huilin, D. Gidaspow, J. Bouillard, L. Wentie, Hydrodynamic simulation of gas–solid flow in a riser using kinetic theory of granular flow, Chemical Engineering Journal, 95 (2003) 1-13.
[33] C.-C. Liao, S.-S. Hsiau, W.-J. Yu, The influence of driving conditions on flow behavior in sheared granular flows, International Journal of Multiphase Flow, 46 (2012) 22-31.